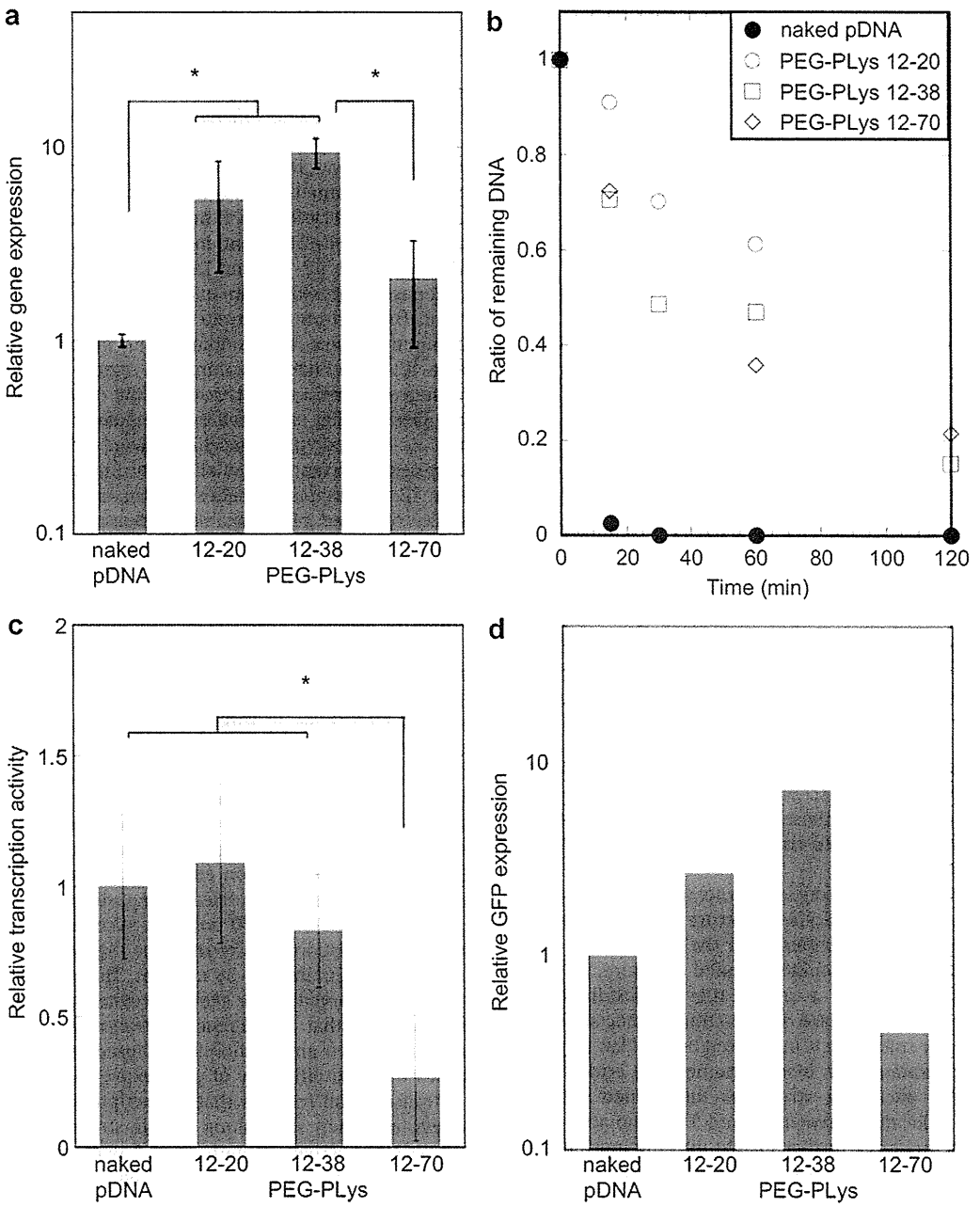

Fig. 3. Biological evaluation of polyplex micelles containing pDNA in different packaging modes. PEG-PLys 12–20 and 12–38 micelles represent folded rod structures whereas 12–70 micelles represent collapsed sphere structures. (a) Gene expression efficiency in the cell-free transcription/translation assay system. Relative light units (RLU) of luciferase expression were normalized to naked pDNA. ($n = 6$, Mean ± SD, $P^* < 0.05$). (b) DNase I degradation as a function of incubation time. (c) *In vitro* transcription efficiency evaluated in a solution containing all elements needed for transcription. The amount of transcribed RNA was normalized to naked pDNA. ($n = 4$, Mean ± SD, $p^* < 0.05$). (d) Gene expression efficiency after cytoplasmic microinjection of naked pDNA and polyplex micelles into Huh-7 cells (100 cells). EGFP gene expression from the polyplex micelles was normalized against that of naked pDNA.

transcription might also be explained simply by the increased DNA binding affinity of the longer cationic PLys segment in 12–70 compared to 12–20 and 12–38, preventing binding and movement of transcription machinery along DNA strands.

Demonstration of improved gene expression in living cells due to the folded packaging of pDNA within polyplex micelles could have significant impacts on therapeutic applications. To examine this possibility, pDNA encoding for EGFP was injected directly into the cytosol of Huh-7-cells either in the naked form or contained in polyplex micelles. As seen in Fig. 3d, enhanced gene expression for 12–20 and 12–38 polyplex micelles compared to naked pDNA was observed, whereas 12–70 polyplex micelles resulted in the lowest expression. This trend correlates well with results obtained in the cell lysate study as shown in Fig. 3a, confirming improved gene expression in the living cell system due to the folded packaging of pDNA. The substantial decrease in gene expression for naked pDNA may be due to nuclease attack and degradation in the cytosol. [22] It is therefore noteworthy to address that enhanced gene

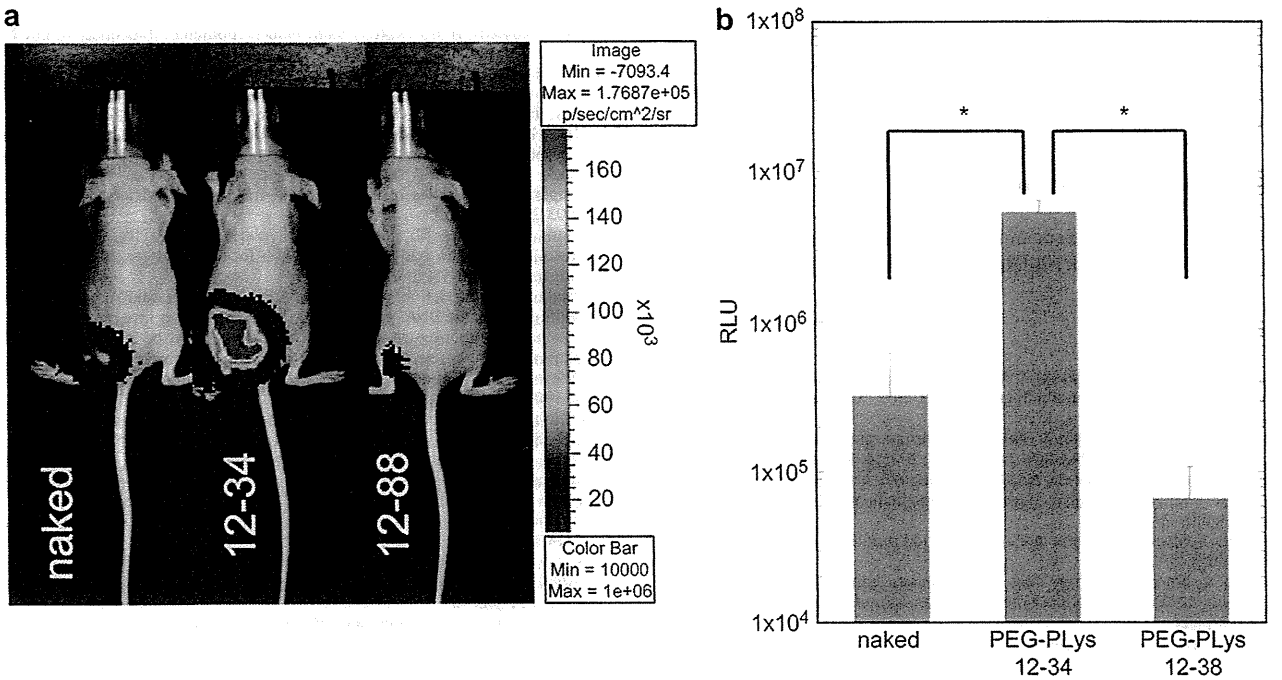

Fig. 4. *In vivo* gene transfer in skeletal muscle following IV injection of naked pDNA or corresponding polyplex micelles during tourniquet application. (a) IVIS images and (b) quantified results ($n = 6$, Mean ± SD. $P^* < 0.05$).

expression demonstrated by folded pDNA packaging may be attributed to its nuclease-tolerability and transcription-active nature.

3.4. Effect of pDNA packaging on in vivo gene expression

Enhanced gene expression due to the folded packaging of pDNA demonstrated in these *in vitro* evaluations motivated us to extend this system to an *in vivo* application. Recently, efficient and safe gene transfer of naked pDNA targeted to skeletal muscle tissue via IV injection in conjunction with a tourniquet was reported. [23,24] Using this method, naked pDNA encoding for luciferase and corresponding polyplex micelles of 12–34 and 12–88, representing folded and collapsed pDNA packaging respectively, were injected into the great saphenous vein of the distal hind limb during temporal tourniquet application. Luciferase expression within skeletal muscle was evaluated by measuring luminescence with an *in vivo* imaging system (IVIS) (Fig. 4). Naked pDNA exhibited significant luciferase expression, which is consistent with the previous report. [23] Gene expression for 12–34 polyplex micelles was much higher than that of naked pDNA, suggesting that enhanced gene expression due to folded packaging occurs even *in vivo*. Significantly lower gene expression was observed for 12–88 polyplex micelles, indicating that controlled packaging of pDNA is critically important for effective gene expression. Targeted gene expression within skeletal muscle is attractive in a practical sense, not only for direct treatment of the diseases in the muscle such as muscular dystrophy, but also as a "protein factory" expressing transgenes continuously and distributing the protein products to the whole body [24–26].

We have previously reported safe and sustained transgene expression in skeletal muscle using the same administration technique used here, and obtained significant tumor growth suppression through the anti-angiogenic effect of the soluble vascular endothelial growth factor (VEGF) receptor-1 (sFlt-1) gene. [24] In that study, 12–16 and 12–38 polyplex micelles exhibited higher gene expression than that of 12–88 polyplex micelles and naked pDNA. This result can now be reasonably understood as the effect of folded pDNA packaging, and concurrently highlights the potential of this packaging formulation for practical therapeutic applications.

4. Conclusions

pDNA packaging within the polyplex micelles was significantly affected by PLys segment length in PEG-PLys block catiomers and two distinct packaging modes were demonstrated, namely, folded packaging through quantized folding and collapsed packaging accompanied by substantial disruption of the double-stranded DNA structure. Higher gene expression resulting from folded pDNA packaging compared to collapsed packaging and naked pDNA was shown not only in a cell-free system and in living cells by cytoplasmic microinjection, but also *in vivo* within skeletal muscle following IV injection. Enhanced gene expression demonstrated by folded pDNA packaging may be attributed to its nuclease-tolerability and transcription-active nature. Results obtained for regularly folded pDNA polyplex micelles were in stark contrast with collapsed pDNA polyplex micelles, probably due to limited transcription efficiency, clearly showing that controlled packaging of pDNA is crucial for achieving effective gene transfer. Promotion of gene transfer through controlled folded packaging of pDNA demonstrates the potential for application of this polyplex micelle system for practical use.

Acknowledgments

This work was financially supported by the Core Research Program for Evolutional Science and Technology (CREST) from the Japan Science and Technology Corporation (JST), by the Japan Society for the Promotion of Science (JSPS) through its "Funding

Program for World-Leading Innovative R&D on Science and Technology (FIRST Program)" and by the Center for Medical System Innovation (CMSI) (Global COE Program, MEXT). The authors also thank Mr. Matthew Pennisi for assistance with manuscript preparation.

Appendix. Supplementary material

Supplementary data associated with this article can be found, in the online version, at doi:10.1016/j.biomaterials.2011.09.046

References

[1] Kataoka K, Harada A, Nagasaki Y. Block copolymer micelles for drug delivery: design, characterization and biological significance. Adv Drug Deliv Rev 2001; 47:113–31.
[2] Pack DW, Hoffman AS, Pun S, Stayton PS. Design and development of polymers for gene delivery. Nat Rev Drug Discov 2005;4:581–93.
[3] Mastrobattista E, van der Aa MAEM, Hennink WE, Crommelin DJA. Artificial viruses: a nanotechnological approach to gene delivery. Nat Rev Drug Discov 2006;5:115–21.
[4] Wagner E, Kloeckner J. Gene delivery using polymer therapeutics. Adv Polym Sci 2006;192:135–73.
[5] Osada K, Kataoka K. Drug and gene delivery based on supramolecular assembly of PEG-polypeptide hybrid block copolymers. Adv Polym Sci 2006; 202:113–53.
[6] Laemmli UK. Characterization of DNA condensates induced by poly(ethylene oxide) and polylysine. P Natl Acad Sci USA 1975;72:4288–92.
[7] Bloomfield VA. DNA condensation. Curr Opin Struct Biol 1996;6:334–41.
[8] Stockmayer WH. Problems of the statistical thermodynamics of dilute polymer solutions. Makromol Chem 1960;35:54–74.
[9] Melnikov SM, Sergeyev VG, Yoshikawa K. Discrete coil-globule transition of large DNA induced by cationic surfactant. J Am Chem Soc 1995;117:2401–8.
[10] Eickbush TH, Moudrianakis EN. Compaction of DNA helices into either continuous supercoils or folded-fiber rods and toroids. Cell 1978;13:295–306.
[11] Kwoh DY, Coffin CC, Lollo CP, Jovenal J, Banaszczyk MG, Mullen P, et al. Stabilization of poly-L-lysine/DNA polyplexes for *in vivo* gene delivery to the liver. Biochim Biophys Acta 1999;1444:171–90.
[12] Katayose S, Kataoka K. Water-soluble polyion complex associates of DNA and poly(ethylene glycol)-poly(L-lysine) block copolymer. Bioconjug Chem 1997; 8:702–7.
[13] Kakizawa Y, Harada A, Kataoka K. Environment-sensitive stabilization of core-shell structured polyion complex micelle by reversible cross-linking of the core through disulfide bond. J Am Chem Soc 1999;121:11247–8.
[14] Itaka K, Yamauchi K, Harada A, Nakamura K, Kawaguchi H, Kataoka K. Polyion complex micelles from plasmid DNA and poly(ethylene glycol)-poly(L-lysine) block copolymer as serum-tolerable polyplex system: physicochemical properties of micelles relevant to gene transfection efficiency. Biomaterials 2003;24:4495–506.
[15] Osada K, Christie RJ, Kataoka K. Polymeric micelles from poly(ethylene glycol)-poly(amino acid) block copolymer for drug and gene delivery. J R Soc Interface 2009;6:S325–39.
[16] Osada K, Oshima H, Kobayashi D, Doi M, Enoki M, Yamasaki Y, et al. Quantized folding of plasmid DNA condensed with block catiomer into characteristic rod structures promoting transgene efficacy. J Am Chem Soc 2010;132:12343–8.
[17] Namork E, Johansen BV. Electron-microscopy of nucleic-acids - effect of different post-treatments on contour-length measurements. Micron 1980;11: 85–90.
[18] Eisenberg H. DNA flexing, folding, and function. Acc Chem Res 1987;20: 276–82.
[19] Osada K, Yamasaki Y, Katayose S, Kataoka K. A synthetic block copolymer regulates S1 nuclease fragmentation of supercoiled plasmid DNA. Angew Chem Int Edit 2005;44:3544–8.
[20] Tinland B, Pluen A, Sturm J, Weill G. Persistence length of single-stranded DNA. Macromolecules 1997;30:5763–5.
[21] Smith SB, Cui YJ, Bustamante C. Overstretching B-DNA: the elastic response of individual double-stranded and single-stranded DNA molecules. Science 1996;271:795–9.
[22] Glasspool-Malone J, Steenland PR, McDonald RJ, Sanchez RA, Watts TL, Zabner J, et al. DNA transfection of macaque and murine respiratory tissue is greatly enhanced by use of a nuclease inhibitor. J Gene Med 2002;4:323–32.
[23] Hagstrom JE, Hegge J, Zhang G, Noble M, Budker V, Lewis DL, et al. A facile nonviral method for delivering genes and siRNAs to skeletal muscle of mammalian limbs. Mol Ther 2004;10:386–98.
[24] Itaka K, Osada K, Morii K, Kim P, Yun SH, Kataoka K. Polyplex nanomicelle promotes hydrodynamic gene introduction to skeletal muscle. J Control Release 2010;143:112–9.
[25] Blau HM, Springer ML. Muscle-mediated gene therapy. N Engl J Med 1995; 333:1554–6.
[26] Lu QL, Bou-Gharios G, Partridge TA. Non-viral gene delivery in skeletal muscle: a protein factory. Gene Ther 2003;10:131–42.

Journal of Controlled Release 155 (2011) 296–302

Contents lists available at ScienceDirect

Journal of Controlled Release

journal homepage: www.elsevier.com/locate/jconrel

Combination of chondroitin sulfate and polyplex micelles from Poly(ethylene glycol)-poly{N'-[N-(2-aminoethyl)-2-aminoethyl]aspartamide} block copolymer for prolonged in vivo gene transfection with reduced toxicity

Satoshi Uchida [a], Keiji Itaka [a,*], Qixian Chen [b], Kensuke Osada [b], Kanjiro Miyata [a], Takehiko Ishii [c], Mariko Harada-Shiba [d], Kazunori Kataoka [a,b,**]

[a] Division of Clinical Biotechnology, Center for Disease Biology and Integrative Medicine, Graduate School of Medicine, The University of Tokyo, 7-3-1 Hongo, Bunkyo-ku, Tokyo, Japan 113-0033
[b] Department of Materials Science and Engineering, Graduate School of Engineering, The University of Tokyo, 7-3-1 Hongo, Bunkyo-ku, Tokyo, Japan 113-0033
[c] Department of Bioengineering, Graduate School of Engineering, The University of Tokyo, 7-3-1 Hongo, Bunkyo-ku, Tokyo, Japan 113-0033
[d] Department of Molecular Pharmacology, National Cerebral and Cardiovascular Center Research Institute, 5-7-1 Fujishiro-dai, Suita, Osaka, Japan 565-8565

ARTICLE INFO

Article history:
Received 7 March 2011
Accepted 27 April 2011
Available online 5 May 2011

Keywords:
Polyplex micelle
Chondroitin sulfate
Gene delivery
Block catiomer
Membrane toxicity

ABSTRACT

Nonviral polycation-based gene carriers (polyplexes) have attracted attention as safe and efficient gene delivery systems. Polyplex micelles comprised of poly(ethyleneglycol)-*block*-poly{N'-[N-(2-aminoethyl)-2-aminoethyl]aspartamide} (PEG-PAsp(DET)) and plasmid DNA (pDNA) have shown high transfection efficiency with low toxicity due to the pH-sensitive protonation behavior of PAsp(DET), which enhances endosomal escape, and their self-catalytic degradability under physiological conditions, which reduces cumulative toxicity during transfection. In this study, we improved the safety and transfection efficiency of this polyplex micelle system by adding an anionic polycarbohydrate, chondroitin sulfate (CS). A quantitative assay for cell membrane integrity using image analysis software showed that the addition of CS markedly reduced membrane damage caused by free polycations in the micelle solution. It also reduced tissue damage and subsequent inflammatory responses in the skeletal muscle and lungs of mice following *in vivo* gene delivery with the polyplex micelles. Subsequently, this led to prolonged transgene expression in the target organs. This combination of polyplex micelles and CS holds great promise for safe and efficient gene introduction in clinical settings.

1. Introduction

Gene therapy has been explored for treating numerous diseases, including genetic disorders and cancers. Cationic polymers are often used for constructing nonviral gene carriers termed polyplexes, due to their advantages, such as large DNA loading capacity, ease of large-scale production, and reduced immunogenicity that has been an issue associated with viral vectors [1–3]. However, an inherent problem with using cationic polymers for gene transfection is their toxicity that causes tissue damage. The positively charged nature of polyplexes can induce nonspecific interactions with anionic biological molecules, such as blood cells, serum proteins, and extracellular matrices, which hinder the efficient delivery of genes, especially for *in vivo* applications.

A promising strategy to resolve these issues is to incorporate a hydrophilic protective layer of poly(ethylene glycol) (PEG) on the surfaces of polyplexes. A polyplex micelle system originally developed by our group is a good example of PEGylated polyplexes. In this system, PEG-polycation block copolymers are complexed with plasmid DNA (pDNA) to form a micellar structure that has a surface with hydrophilic and electrically neutral PEG and an inner core containing pDNA in a condensed state [4–8]. This structure increases the steric stability of the polyplexes under physiological conditions and exhibits less nonspecific interactions with biological components, such as serum proteins. In addition, a new polycation, poly{N'-[N-(2-aminoethyl)-2-aminoethyl]aspartamide} (PAsp(DET)), used as a core-forming segment of polyplex micelles, was developed to increase transfection efficiency [6].

Comprehensive analyses revealed that the high gene transfection capability of PAsp(DET) was mainly attributed to two distinct properties: (1) pH-responsive change in the degree of protonation, which enhanced endosomal escape [9] and (2) self-catalytic degradability under physiological conditions, which reduced the cumulative toxicity during transfection [10]. Using PEG-PAsp(DET) block copolymers, we achieved effective and sustained transgene expressions for *in vivo* local administration [11] and succeeded in bone

* Correspondence to: K. Itaka, Division of Clinical Biotechnology, Center for Disease Biology and Integrative Medicine, Graduate School of Medicine, The University of Tokyo, 7-3-1 Hongo, Bunkyo-ku, Tokyo 113-0033, Japan. Tel.: +81 3 5841 1418; fax: +81 3 5841 1419.
** Correspondence to: K. Kataoka, Department of Materials Engineering, Graduate School of Engineering, The University of Tokyo, 7-3-1 Hongo, Bunkyo-ku, Tokyo 113-0033, Japan. Tel.: +81 3 5841 7138; fax: +81 3 5841 7139.
E-mail addresses: itaka-ort@umin.ac.jp (K. Itaka), kataoka@bmw.t.u-tokyo.ac.jp (K. Kataoka).

0168-3659/$ – see front matter © 2011 Elsevier B.V. All rights reserved.
doi:10.1016/j.jconrel.2011.04.026

regeneration by introducing osteogenic factor-expressing genes for bone defects in the mouse skull [8].

These PEG-PAsp(DET)/pDNA polyplex micelles (PMs) were applied to bone defect areas after their incorporation into a scaffold. Among several scaffolds tested, a commercial calcium phosphate paste (BIOPEX-R; Mitsubishi Pharma, Osaka, Japan) yielded the highest transgene expression. BIOPEX-R contains a considerable amount of chondroitin sulfate (CS), an anionic polycarbohydrate. This result led us to hypothesize that CS might play a critical role in gene introduction using PMs.

This study was designed to verify this hypothesis. We sought to identify the mechanisms involved with improved transfection after the addition of CS to PMs using physicochemical analyses, *in vitro* transfection, and *in vivo* local gene transfer.

2. Materials and methods

2.1. Materials

Plasmid DNA (pDNA) encoding luciferase (pGL4.13: Promega, Madison, WI) was amplified in competent DH5α *Escherichia coli* and purified using NucleoBond Xtra EF (Nippon Genetics, Tokyo, Japan). The pDNA concentration was determined from the absorbance at 260 nm. Dulbecco's modified Eagle's medium was from Sigma-Aldrich (St. Louis, MO, USA) and fetal bovine serum was from Dainippon Sumitomo Pharma Co., Ltd. (Osaka, Japan). Chondroitin sulfate A (CS) was from Sigma-Aldrich. Linear polyethyleneimine (LPEI) (Exgen 500; MW = 22 kDa) was from MBI Fermentas (Burlington, ON, Canada).

2.2. Animals

ICR mice (female, 7 weeks old) were purchased from Charles River Laboratories. All animal protocols were conducted with the approval of the Animal Care and Use Committee of the University of Tokyo.

2.3. Preparation of polyplex micelle solutions

PEG-PAsp(DET) block copolymer was synthesized as previously reported [6]. The PEG used had a molecular weight of 12,000 and the polymerization degree of the PAsp(DET) portion was determined to be 69 by ^{1}H-NMR. PEG-PAsp(DET) block copolymers and pDNA were separately dissolved in 10 mM Tris–HCl buffer (pH 7.4). PEG-PAsp (DET)/pDNA polyplex micelles (PMs) were obtained by simply mixing both solutions. After mixing for 10 min, PEG-PAsp(DET)/pDNA/CS polyplex micelles (CS-PMs) were prepared by adding CS at varying concentrations. In this study, the residual molar ratio of amino groups in PEG-PAsp(DET), phosphate groups in pDNA, and the total carboxyl and sulfate groups in CS was defined as N:P:CS. The final pDNA concentration was adjusted to 30 μg/ml for *in vitro* experiments and 133 μg/ml for *in vivo* experiments.

2.4. Luciferase expression and cell viability after transfection of PMs and CS-PMs

Cells were seeded at a density of 5000 cells/well in a 96-multiwell plate and cultured for 24 h. After the culture medium was replaced with fresh medium containing 10% fetal bovine serum, PMs or CS-PMs containing 0.18 μg pDNA was added to each well. Firefly luciferase expression was determined using a Luciferase assay system (Promega, Madison, WI, USA) and a GloMaxTM 96 microplate luminometer (Promega) following the manufacturer's protocol. Cell viability was determined using a Cell Counting Kit-8 (Dojindo, Kumamoto, Japan) following the manufacturer's protocol.

2.5. Quantitative assay for the cellular uptake of pDNA

Cells were seeded at a density of 80,000 cells/well in a 6-multiwell plate and transfection was performed as in the previous section using 4 μg pDNA/well. Plasmid DNA was collected and purified from each well using a Wizard Genomic DNA purification kit (Promega). Purified DNA was then subjected to real time polymerase chain reaction (PCR) for the quantification of pDNA copies encoding Luc2 using an ABI Prism 7500 Sequence Detector (Applied Biosystems, Foster City, CA) and the following primers: forward primer GGACTTGGACACCGG-TAAGA and reverse primer GTCGAAGATGTTGGGGTGTT. The copy number of β-actin was also determined by TaqMan Gene Expression Assays (Applied Biosystems) to normalize the cell number.

2.6. Evaluation of cell membrane integrity

Cells were seeded at a density of 10,000 cells/well in a 48-multiwell plate and cultured for 24 h. After the culture medium was replaced with PBS, PMs or CS-PMs containing 0.5 μg pDNA was added to each well. The cells were treated with 1 μM YO-PRO1 and 2.5 μg/ml Hoechst 33342 in phosphate buffered saline (PBS) 30 min later. Ten minutes later, the fluorescent intensity of each nucleus was quantitatively evaluated using a fluorescence microscope equipped with image-analysis software (IN Cell Analyzer 1000: GE Healthcare UK Ltd., Buckinghamshire, England).

2.7. Fluorescent labeling of PEG-PAsp(DET)

Alexa680-NHS (Invitrogen, Carlsbad, CA) was conjugated to the amino groups of PEG-PAsp(DET). PEG-PAsp(DET) was dissolved in 0.1 M $NaHCO_3$ at 4 °C, and an equimolar amount of Alexa680 in dimethylformamide (DMF) solution was added. After reacting for 3 h at 4 °C, the mixture was first dialyzed against an aqueous solution of 0.001 N HCl, and then against de-ionized water in dialysis tubing (MWCO: 12–14 kDa). The number of Alexa680 molecules conjugated to each PEG-PAsp(DET) molecule was determined to be 0.79 from the absorbance at 680 nm.

2.8. Fluorescence correlation spectroscopic (FCS) measurements of PEG-PAsp(DET)/CS mixtures

Alexa680-labeled PEG-PAsp(DET) solution at a concentration of 1 mg/ml and an equal volume of CS solution at varying concentrations was mixed and then diluted 30 times with PBS (pH 7.4) and MES buffer (pH 5.5) containing 20 mM MES and 150 mM NaCl, respectively. FCS measurements used a ConfoCor3 module (Carl Zeiss, Jena, Germany) equipped with a Zeiss C-Apochromat 40× water objective. A He–Ne laser (633 nm) was used for Alexa680-labeled pDNA excitation. For each sample, measurements were performed at room temperature with a sampling time of 20 s and repeated 10 times.

For the quantification of free PEG-PAsp(DET), a two-component model was applied to autocorrelation curves, where one component was free PEG-PAsp(DET) and the other was CS/PEG-PAsp(DET) complexes. When using this model, the diffusion times for free PEG-PAsp(DET) and CS/PEG-PAsp(DET) complexes were fixed. The diffusion time for CS/PEG-PAsp(DET) complexes was measured at CS:N = 1:1, because the diffusion time reached a plateau at a CS:N ratio of 0.5 at pH 7.4 and at a ratio of 1 at pH 5.5.

2.9. Förster resonance energy transfer (FRET) measurements

Double labeling of pDNA using fluorescein (ex/em = 492/518 nm) and Cy3 (550/570 nm) was done using Label IT Tracker Intracellular Nucleic Acid Localization Kits (Mirus) with a slightly modified protocol. The spectral properties of the pDNA were evaluated using a NanoDrop ND-3300 fluorospectrometer (NanoDrop Technologies,

Wilmington, DE) at an excitation of 470 nm with a blue LED. FRET efficiency was calculated from the relative emission ratio of Cy-3 (567 nm) to fluorescein (523 nm).

2.10. Size measurements of PMs by FCS

Plasmid DNA was labeled using Label IT Tracker Intracellular Nucleic Acid Localization Kits (Mirus, WI) following the manufacturer's protocol. The final DNA concentration was adjusted to 1.5 μg/ml. FCS measurements were performed as described previously. A He–Ne laser (633 nm) was used for Cy-5-labeled pDNA excitation.

2.11. Z-potential

Zeta potential was determined using a Zetasizer (Malvern Instruments, Worcestershire, U.K.) with a He–Ne Laser (λ = 633 nm) for the incident beam at a detection angle of 173° and at a temperature of 25 °C.

2.12. Intratracheal gene introduction into the lung

Mice were anesthetized by intraperitoneal administration of pentobarbital (60 mg/kg) (Kyoritsu Seiyaku, Tokyo, Japan). A microsprayer Model IA-1C-R (Penn Century, Philadelphia, PA) was placed into the trachea through the mouth, and then 50 μl of PM or CS-PM solution containing 6.7 μg pDNA was administered. Bronchoalveolar lavage (BAL) was performed with 500 μl PBS (instilled and recovered 4 times). LDH in BAL fluid was determined using a QuantiChrom Lactate Dehydrogenase Kit (BioAssay Systems, Hayward, CA) following the manufacturer's protocol. For mRNA measurements, lung tissue was extracted and total RNA was isolated using an RNeasy Mini Preparation Kit (Qiagen, Hilden, Germany) following the manufacturer's protocol. Gene expression was analyzed by real-time quantitative PCR using TaqMan Gene Expression Assays and an ABI Prism 7500 Sequence Detector. An IVIS™ Imaging System (Xenogen, Alameda, CA) was used to evaluate luciferase expression in the lung after intravenous injection of D-luciferin following the manufacturer's protocol.

2.13. Hydrodynamic gene introduction into skeletal muscle

Hydrodynamic gene introduction into skeletal muscle was performed as previously reported [12]. Briefly, after anesthetizing mice with 3% isoflurane (Abbott Japan Co., Ltd., Tokyo, Japan), a tourniquet was placed on the proximal thigh to transiently restrict blood flow. Then, from a distal site of the great saphenous vein, naked pDNA, PM, or CS-PM solution (375 μl) containing 50 μg pDNA was injected in 5 s. At 5 min after injection, the tourniquet was released. Blood samples were collected from the *vena cava* and allowed to stand overnight at 4 °C, followed by centrifugation to obtain serum. Serum CPK was determined using an Enzychrom Creatine Kinase Assay kit (BioAssay Systems) following the manufacturer's protocol. An IVIS™ Imaging System was used to evaluate luciferase expression in muscle after intravenous injection of D-luciferin.

3. Results and discussion

3.1. In vitro transfection with chondroitin sulfate

Cultured cell lines were transfected by PEG-PAsp(DET)/pDNA polyplex micelles (PMs) in the presence of chondroitin sulfate (CS). As the optimized charge ratio of PEG-PAsp(DET): pDNA is N:P = 80:1 [6,8], PEG-PAsp(DET)/pDNA/CS polyplex micelle systems (CS-PMs) were constructed by adding CS to PM solutions at the charge ratios of PEG-PAsp(DET): pDNA: CS (N:P:CS) = 80:1:10 and 80:1:100, in which the CS charge was calculated as the total number of carboxylate and sulfate residues. As shown in Fig. 1A, CS-PMs induced higher transgene expression in NIH3T3 cells than PMs alone. Other cell lines also showed similar enhancements in transgene expressions by the addition of CS, although the optimal amount of CS differed depending on the cell line (Supplementary Fig. 1). Interestingly, although the final transgene expressions improved with CS, an evaluation of the time-dependent change revealed that CS addition induced a delay in the time to achieve maximal transgene expression, which was in good agreement with the delayed profile in cellular uptake of CS-PMs (Fig. 1B, C).

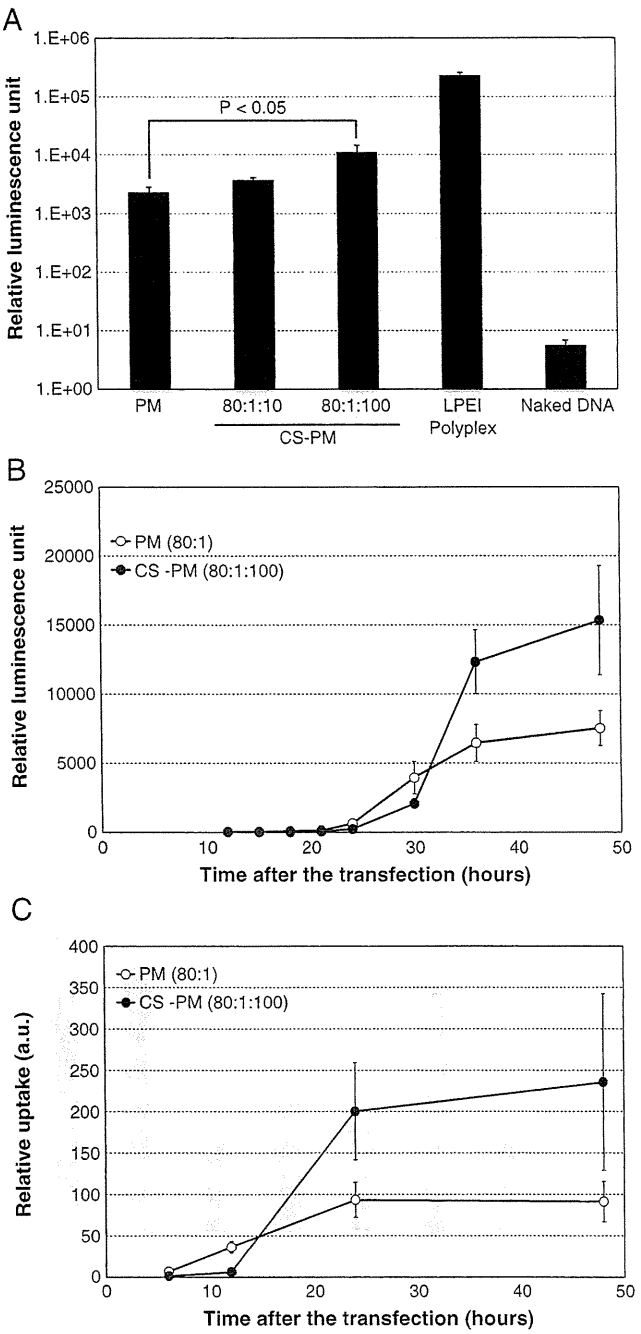

Fig. 1. Transfection efficiency in vitro. PM (N:P = 80:1), CS-PM (N:P:CS = 80:1:10 and 80:1:100), LPEI (N:P = 10:1) and naked DNA were transfected into NIH3T3 cells. A. Luciferase expressions after 48 h. B. Time-dependent profiles of luciferase expressions. C. Time-dependent profiles of pDNA uptake measured by quantitative PCR. Results are means ± SEMs (n = 5).

The PMs examined here, as well as most other polycation-based gene delivery systems, require an excess ratio of cationic polymers to pDNA for efficient transfection [6,8]. It is reasonable to assume that, at such a high N:P ratio, a considerable amount of PEG-PAsp(DET) exists in the free state without binding to PMs. Several reports have argued that free cationic polymers may be involved in endosomal escape and intracellular trafficking [13,14]. However, a critical issue is that these free polymers may induce toxic effects by interacting with cell membranes and other anionic biocomponents. It is possible that the anionic polycarbohydrate CS might abrogate such toxicity by associating with free polycations. Indeed, several recent studies that focused on the addition of polyanions, including CS, to polyplex systems showed enhanced transfection efficiency and reduced toxicity [15–20].

Accordingly, we analyzed the effect of CS on cell membrane integrity during *in vitro* transfection of PMs or CS-PMs. To assess cell membrane integrity, we used a DNA intercalator, YO-PRO1, which is impermeable to the normal cell membrane, but will permeate a membrane with perturbed integrity and emit a strong fluorescent signal due to DNA intercalation [21]. The fluorescent intensities of cultured cells due to permeated YO-PRO1 were quantitatively evaluated with a fluorescence microscope equipped with image-analysis software (IN Cell Analyzer 1000: GE Healthcare UK Ltd.).

At 30 min after transfection, the PMs formed at N:P = 80:1 induced an increase in fluorescent signals of YO-PRO1, suggesting enhanced cell membrane permeability (Fig. 2). In contrast, the PMs prepared at N:P = 3:1 showed almost no increase compared to the control. As reported previously, there was a substantial increase in the amount of free PEG-PAsp(DET) in the PM solution at an increased N:P [22]. Thus, it was reasonable to assume that the free PEG-PAsp(DET) in medium may have been involved in this significant increase in membrane permeability observed for the PM system at high N:P.

Indeed, addition of a corresponding amount of free PEG-PAsp (DET) into the medium induced as great an increase in fluorescence as the PMs prepared at N:P = 80:1, which was consistent with the previous assumption. Although polyplex from linear polyethyleneimine (LPEI) (N:P = 10), a commonly used transfectant, showed higher transfection efficiency than PMs or CS-PMs (Fig. 1A), the membrane damage and the cytotoxicity were notably observed for this system (Fig. 2 and Supplementary Fig. 2). In contrast, the membrane damage was substantially lowered in PEG-PAsp(DET) compared to PEI, indicating that the damage was sufficiently modest to have been effectively abrogated by the addition of CS. It should be noted that the enhanced cell membrane permeability was a transient, reversible phenomenon only at the initial phase of transfection, as it was not observed at 24 h after transfection (data not shown). Cell viabilities evaluated by an MTT assay at 48 h after transfection remained at nearly 100%, regardless of the presence or absence of CS (Supplementary Fig. 2).

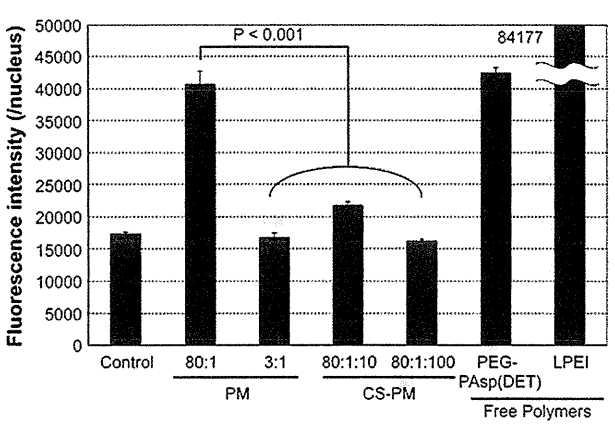

Fig. 2. Evaluation of membrane destabilization *in vitro*. PMs (N:P = 3:1 and 80:1), CS-PMs (N:P:CS = 80:1:10 and 80:1:100), and free PEG-PAsp(DET) and linear polyethyleneimine (LPEI)) with the same amine concentration as PMs (N:P = 80:1) were added to NIH3T3 cells, followed by treatment with YO-PRO1. The mean fluorescence intensity in cell nuclei was quantified for each well. About 3000 cells were analyzed in each well. Results are means of 3 wells ± SEMs.

3.2. Physicochemical characterization of CS-modulated polyplex systems

Next, we analyzed the effect of CS addition on the behaviors of free polycations as well as PMs. The reduced membrane damage after CS addition suggested that the amount of free polycations may have been substantially decreased in CS-PM solution due to the formation of polyion complexes between CS and excess PEG-PAsp(DET) in the medium.

Thus, to analyze the state of PEG-PAsp(DET) after mixing with varying ratios of CS, we measured the diffusion properties of Alexa680-labeled PEG-PAsp(DET) using FCS.

The diffusion time for PEG-PAsp(DET) reached a plateau at a CS:N ratio of 0.5:1, where the number of CS anionic charges was nearly equal to that of the PEG-PAsp(DET) cationic charges; approximately half of the amino groups in the 1,2-diaminoethane units in the side chain are protonated at pH 7.4 [9], suggesting the formation of a stoichiometric complex of CS and PEG-PAsp(DET) (Fig. 3). This result also suggested that there would be no free PEG-PAsp(DET) in the solution at CS:N ratios >0.5.

The formation of a stoichiometric complex around CS:N = 0.5:1 was also confirmed by measuring the z-potential (Supplementary Fig. 3). While the complex prepared at CS:N = 0.5:1 had a single fraction at around a neutral charge, the complex at CS:N = 1:1 had another fraction around −30 mV corresponding to free CS. Further, DLS measurements revealed that the CS/PEG-PAsp(DET) complex that was formed had a size of 43 nm with a narrow distribution of polydispersity index (PDI) = 0.13, indicating the formation of polyion complex micelles with a CS/PAsp(DET) core surrounded by a PEG shell. Of note is that the CS-PM system, even without free polycations, yielded a higher transfection efficiency than PM alone, as shown in Fig. 1A. We will return to this matter in a subsequent section of this paper.

Next, we examined the physicochemical properties of PMs with or without CS. For this purpose, we used a charge ratio of N:P = 20:1, because too great an excess of cationic polymers may interfere with precise analyses of the PMs characteristics. Because CS has an anionic nature, there may be a possibility of loosening the condensed structure of PMs [23]. The condensed state of DNA was analyzed by FRET measurements using DNA labeled with a pair of donor–acceptor fluorescent dyes on a single DNA molecule [24,25]. Of interest is that even with the addition of CS, there was no significant change in the

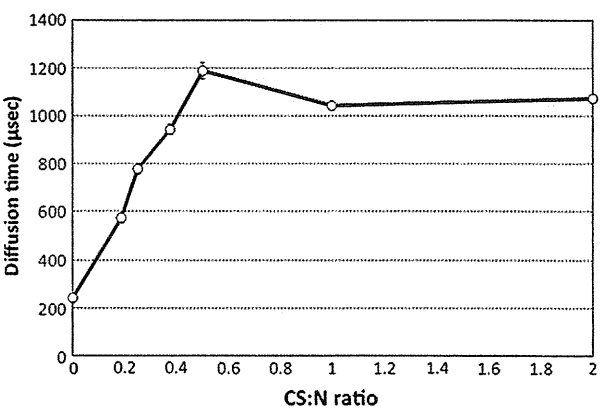

Fig. 3. Diffusion time measurements for Alexa680-labeled PEG-PAsp(DET) by FCS in the presence of varying amounts of CS in the solution. Results are means ± SDs.

condensation state of pDNA, suggesting that the disintegration of PM may not occur even in the presence of an appreciable amount of CS (Fig. 4). FCS using Cy5-labeled pDNA revealed that the diffusion time, which is proportional to particle diameter, showed a slight increase of approximately 1.3-fold after the addition of CS, suggesting some portion of CS may undergo the interaction with PMs (Fig. 5). The PMs z-potential became slightly negative after the addition of CS (+1.5 mV → −5.5 mV). These results suggested that the interaction of CS caused slight changes in the diameter and z-potential of PMs, although the PM structure with condensed pDNA in the core remained stable.

3.3. *In vivo* gene delivery into lung and skeletal muscle

To confirm the effect of CS for *in vivo* conditions, we performed transfection into mouse lung via intratracheal administration. To evaluate tissue damage, we quantified LDH released into bronchoalveolar lavage fluid (BALF) at 30 min after the administration. As shown in Fig. 6, CS significantly reduced LDH release to a level comparable to that of untreated mice. We also assessed the consequent tissue damage by quantifying the mRNA levels of pro-inflammatory cytokines in lung tissue at 24 h after administration. Although PMs induced a low, but detectable upregulation of TNF-α and Cox-2, CS addition significantly reduced the production of these cytokines (Fig. 7). Interestingly, the luciferase expressions evaluated by an IVIS Imaging System were comparable for these two systems with or without CS (Fig. 8).

Another *in vivo* approach is by using a hydrodynamic injection that targets skeletal muscle [12]. To assess toxicity, serum creatine phosphokinase (CPK) was determined at 4 h after injection. Using CS-PMs, the CPK level was significantly reduced compared to PMs, suggesting that CS also reduced the tissue damage in muscles (Fig. 9). In addition, CS-PMs yielded a higher and more prolonged transgene expression compared to PMs and naked pDNA, although there was no statistically significant difference among these 3 groups (Fig. 10). These *in vivo* results indicated that CS exhibited the favorable effects of ameliorating tissue damage and reducing the inflammatory response at the injection site without affecting the transfection competency of PMs.

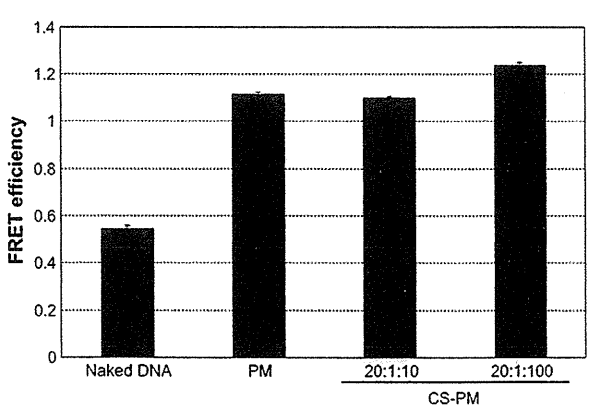

Fig. 4. Evaluation of pDNA condensation in the polyplexes by Förster resonance energy transfer (FRET). FRET efficiency between a pair of donor-acceptor fluorescent dyes (fluorescein and Cy3) tagged onto pDNA was determined for naked pDNA, PMs (N:P = 20:1), and CS-PMs (N:P:CS = 20:1:10 and 20:1:100). FRET efficiency is expressed as the emission intensity ratio of 567 nm (Cy3 emission) to 523 nm (fluorescein emission), where a higher value indicates a more condensed state of pDNA in the polyplexes. Results are means ± SDs (n = 3).

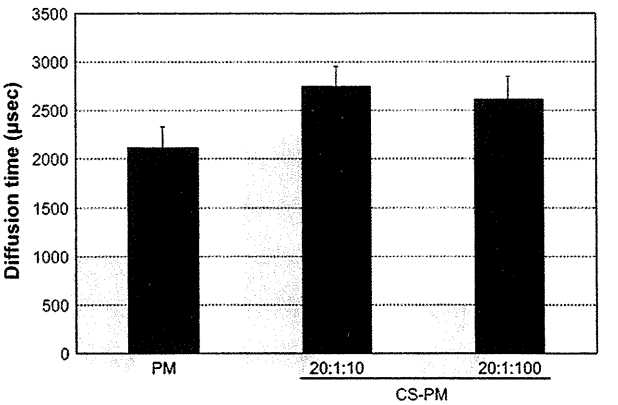

Fig. 5. Diffusion times for PMs (N:P = 20:1) and CS-PMs (N:P:CS = 20:1:10 and 20:1:100) measured by FCS. Results are means ± SDs.

3.4. Possible mechanisms for CS that improve the gene transfection efficacy of PM systems

The PM systems examined here consisted of a PEG-based block catiomer, PEG-PAsp(DET), which significantly reduced the cellular toxicity compared to polyplexes using non-PEGylated polycations [10,11]. Indeed, PM addition into the culture medium resulted in no decreases in cell viability as assessed by MTT assays (Supplementary Fig. 2). Nevertheless, a more sensitive assay to evaluate cell membrane integrity revealed that there was putative damage that increased membrane permeability, even though this was transient, and resulted in YO-PRO1 intercalated into chromosomal DNA to emit a fluorescent signal (Fig. 2). Worth noting is that this membrane damage was successfully abrogated by the addition of CS.

This was apparently due to neutralizing free polycations, the main component considered to cause membrane damage, in the medium via polyion complex formation. It is also worth noting that this propensity of CS to reduce membrane damage of the cultured cells caused by polycations is in line with the reduced adverse effects observed *in vivo*, including inflammatory cytokine production and tissue damage that induces LDH release. Thus, the use of CS in clinical settings is appealing for increasing the compliance of these PM systems. Although previous studies focused on the effects of anionic polycarbohydrates, such as hyaluronic acid (HA) and CS, on the behavior of cationic polylpexes [15–20], few of them addressed their roles in scavenging toxic free polycations.

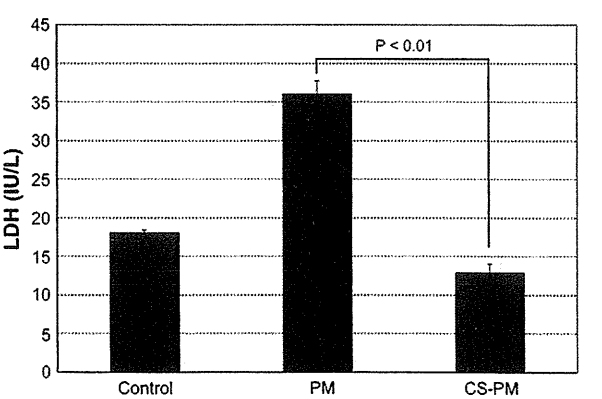

Fig. 6. LDH activity in bronchoalveolar lavage fluid (BALF). BALF was collected 30 min after the intratracheal administration of PMs (N:P = 20:1) and CS-PMs (N:P:CS = 20:1:100). Control indicates an untreated group. Results are means ± SEMs (n = 3).

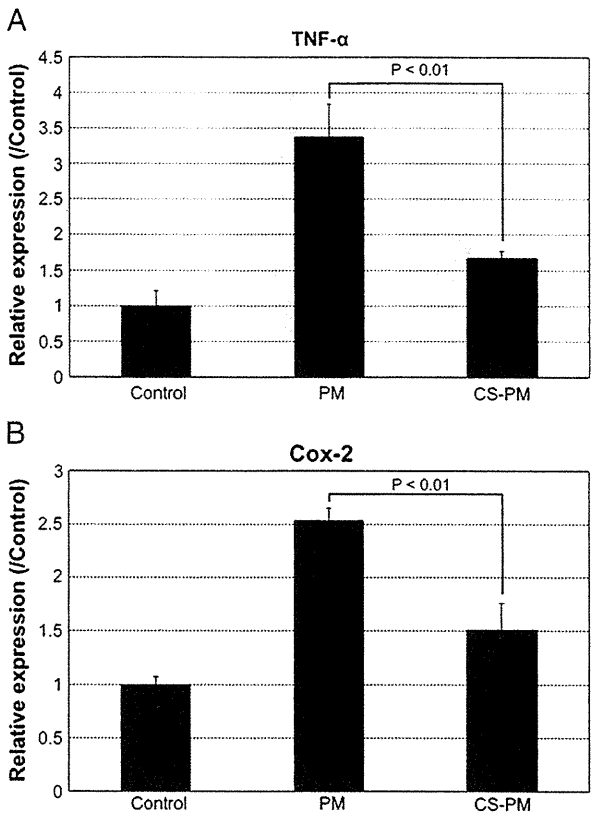

Fig. 7. Evaluation of pro-inflammatory cytokine (TNF-α and Cox-2) expression in lung tissue. PMs (N:P = 20:1) and CS-PMs (N:P:CS = 20:1:100) were administered intratracheally. Messenger RNA expression in lung was measured by quantitative polymerase chain reaction (PCR) at 24 h after administration. A. TNF-α, B. Cox-2. Results indicate relative values to untreated controls (means ± SEMs; n = 4).

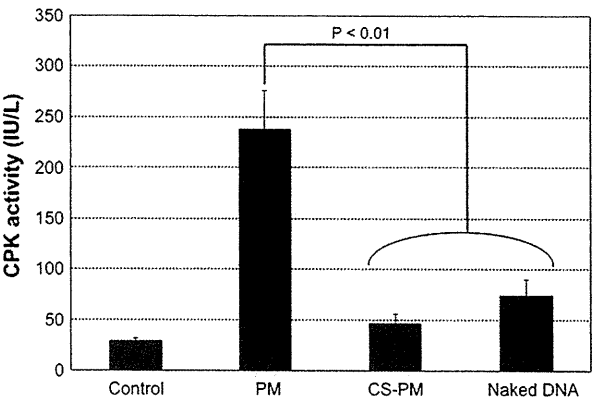

Fig. 9. Quantification of serum creatine phosphokinase (CPK). Serum was collected at 4 h after hydrodynamic injection of naked pDNA, PMs (N:P = 20:1), and CS-PMs (N:P:CS = 20:1:100). Control indicates an untreated group. Results are means ± SEMs (n = 5).

The primary reason for requiring excess polycations in their free form in the polyplex system is that these free polycations are assumed to be internalized into endosomes along with the polyplexes, thus facilitating their escape from endosomes to the cytoplasm by a proton sponge effect and/or direct perturbation of endosomal membranes. In any case, masking free polycations with CS via complexation is unfavorable for promoting endosomal escape, and is inconsistent with the observed preservation, or even improvement, in transfection efficacy of CS-PMs both *in vitro* and *in vivo*.

A plausible explanation for this controversial phenomenon is to assume a rearrangement of CS/PEG-PAsp(DET) complex micelles within endosomes that is synchronized with a pH drop to release free PEG-PAsp(DET). Note that, as shown in Fig. 3, CS/PEG-PAsp(DET) complex micelles have a charge stoichiometric composition of CS:N = 0.5:1 at pH 7.4. Thus, to maintain the charge stoichiometric regime, even at a lowered pH, there should be a liberation of a certain fraction of PEG-PAsp(DET) from the micelles. The pKa for the second protonation of the 1,2-diaminoethane unit of PAsp(DET) is 6.3 [9]. The endosomal pH, in turn, is reported to be ≈5.0–5.5, so that eventually PAsp(DET) in this pH range undergoes an additional protonation in the 1,2-diaminoethane unit, resulting in a shift in the charge stoichiometric ratio from CS:N = 0.5:1 to 1:1 and drives the liberation of PEG-PAsp(DET) from the micelles for charge compensation.

To estimate the pH responsive release of free PEG-PAsp(DET), we used FCS measurements for mixed solutions of CS and Alexa680-labeled PEG-PAsp(DET). As expected, a substantial amount of free PEG-PAsp(DET) was found at a CS:N = 0.5:1 at pH 5.5, which was consistent with the assumed liberation of PEG-PAsp(DET) from the complex micelles at the lowered pH conditions of the endosome

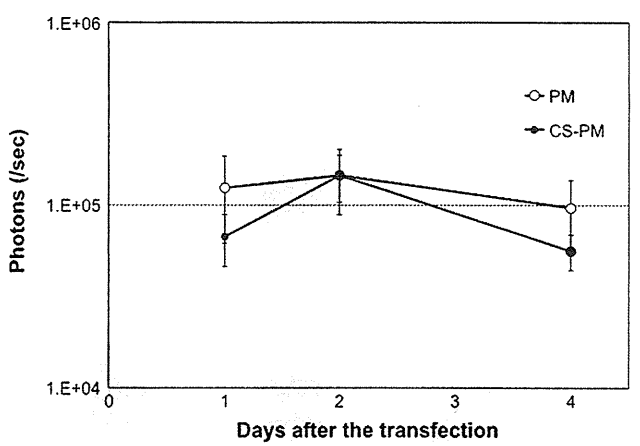

Fig. 8. Luciferase expressions in lung after intratracheal administration. PMs (N:P = 20:1;open circles) and CS-PMs (N:P:CS = 20:1:100; closed circles) loaded with a luciferase-expressing gene were administered intratracheally. The time-dependent profiles of luciferase gene expression were measured with an IVIS Imaging System. Results are means ± SEMs (n = 4).

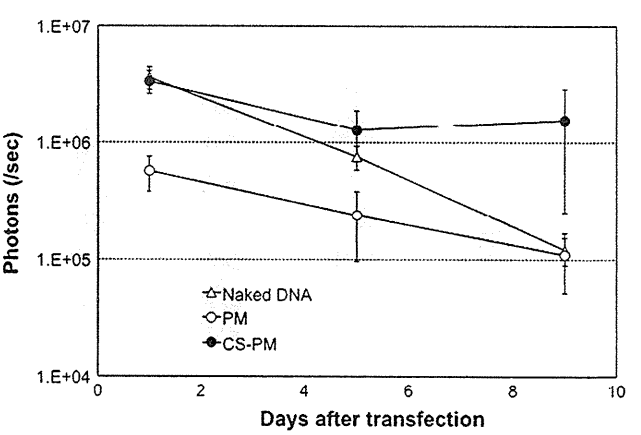

Fig. 10. Transfection efficacy in muscle after hydrodynamic injection. Naked pDNA (open triangles), PMs (N:P = 20:1; open circles), and CS-PMs (N:P:CS = 20:1:100; closed circles) were hydrodynamically injected into a hind limb muscle. The time-dependent profiles of luciferase gene expression were measured with an IVIS Imaging System. Results are means ± SEMs (n = 5).

(Supplementary Fig. 4). Worth noting is that the amount of free polymers became negligible at CS:N = 1:1 and pH 5.5, which supports the formation of a charge stoichiometric complex of CS with fully protonated PEG-PAsp(DET).

Consequently, from the above estimations, it is reasonable to conclude that the cellular uptake of CS/PEG-PAsp(DET) complex micelles along with CS-PMs enhances the endosomal escape of CS-PMs by releasing free PEG-PAsp(DET) in endosomes, leading to a high transfection efficiency.

4. Conclusions

The addition of CS to PEG-PAsp(DET)/DNA polyplex micelles abrogated membrane damage after *in vitro* and *in vivo* gene transfection. Effective complexation of CS with free polymers prevented the nonspecific binding to and the resulting destabilization of cell membranes. Further, CS/PEG-PAsp(DET) complex micelles co-localized in endosomes with CS-PMs selectively liberate free PEG-PAsp(DET) in the acidic compartment of the endosome, thereby facilitating the cytoplasmic translocation of CS-PMs and leads to effective gene expression. During *in vivo* gene transfer, CS remarkably reduced the inflammatory responses and tissue damage at the injection site. Thus, this system of PEG-PAsp(DET)/DNA polyplex micelles combined with CS shows promise for safe and practical gene transfer in future clinical settings.

Supplementary materials related to this article can be found online at doi:10.1016/j.jconrel.2011.04.026.

Acknowledgements

This work was financially supported in part by the Core Research Program for Evolutional Science and Technology (CREST) from Japan Science and Technology Corporation (JST) (K. K.), Grants-in-Aid for Scientific Research form the Japanese Ministry of Education, Culture, Sports, Science and Technology, Japan (MEXT) (K. I.), and Global COE Program "Medical System Innovationon through Multidisciplinary Integration" from MEXT, Japan. We thank Satomi Ogura, Yoko Hasegawa and Katsue Morii (The University of Tokyo) for technical assistance.

References

[1] S.C. De Smedt, J. Demeester, W.E. Hennink, Cationic polymer based gene delivery systems, Pharm. Res. 17 (2) (2000) 113–126.
[2] D. Schaffert, E. Wagner, Gene therapy progress and prospects: synthetic polymer-based systems, Gene Ther. 15 (16) (2008) 1131–1138.
[3] K. Itaka, K. Kataoka, Recent development of nonviral gene delivery systems with virus-like structures and mechanisms, Eur. J. Pharm. Biopharm. 71 (3) (2009) 475–483.
[4] S. Katayose, K. Kataoka, Water-soluble polyion complex associates of DNA and poly(ethylene glycol)-poly(L-lysine) block copolymer, Bioconjug. Chem. 8 (5) (1997) 702–707.
[5] K. Itaka, K. Yamauchi, A. Harada, K. Nakamura, H. Kawaguchi, K. Kataoka, Polyion complex micelles from plasmid DNA and poly(ethylene glycol)-poly(L-lysine) block copolymer as serum-tolerable polyplex system: physicochemical properties of micelles relevant to gene transfection efficiency, Biomaterials 24 (24) (2003) 4495–4506.
[6] N. Kanayama, S. Fukushima, N. Nishiyama, K. Itaka, W.D. Jang, K. Miyata, Y. Yamasaki, U.I. Chung, K. Kataoka, A PEG-based biocompatible block catiomer with high buffering capacity for the construction of polyplex micelles showing efficient gene transfer toward primary cells, ChemMedChem 1 (4) (2006) 439–444.
[7] K. Osada, H. Oshima, D. Kobayashi, M. Doi, M. Enoki, Y. Yamasaki, K. Kataoka, Quantized folding of plasmid DNA condensed with block catiomer into characteristic rod structures promoting transgene efficacy, J Am Chem Soc 132 (35) (2010) 12343–12348.
[8] K. Itaka, S. Ohba, K. Miyata, H. Kawaguchi, K. Nakamura, T. Takato, U.I. Chung, K. Kataoka, Bone regeneration by regulated in vivo gene transfer using biocompatible polyplex nanomicelles, Mol. Ther. 15 (9) (2007) 1655–1662.
[9] K. Miyata, M. Oba, M. Nakanishi, S. Fukushima, Y. Yamasaki, H. Koyama, N. Nishiyama, K. Kataoka, Polyplexes from poly(aspartamide) bearing 1,2-diaminoethane side chains induce pH-selective, endosomal membrane destabilization with amplified transfection and negligible cytotoxicity, J. Am. Chem. Soc. 130 (48) (2008) 16287–16294.
[10] K. Itaka, T. Ishii, Y. Hasegawa, K. Kataoka, Biodegradable polyamino acid-based polycations as safe and effective gene carrier minimizing cumulative toxicity, Biomaterials 31 (13) (2010) 3707–3714.
[11] M. Harada-Shiba, I. Takamisawa, K. Miyata, T. Ishii, N. Nishiyama, K. Itaka, K. Kangawa, F. Yoshihara, Y. Asada, K. Hatakeyama, N. Nagaya, K. Kataoka, Intratracheal gene transfer of adrenomedullin using polyplex nanomicelles attenuates monocrotaline-induced pulmonary hypertension in rats, Mol. Ther. 17 (7) (2009) 1180–1186.
[12] K. Itaka, K. Osada, K. Morii, P. Kim, S.H. Yun, K. Kataoka, Polyplex nanomicelle promotes hydrodynamic gene introduction to skeletal muscle, J. Control. Release 143 (1) (2010) 112–119.
[13] S. Boeckle, K. von Gersdorff, S. van der Piepen, C. Culmsee, E. Wagner, M. Ogris, Purification of polyethylenimine polyplexes highlights the role of free polycations in gene transfer, J. Gene Med. 6 (10) (2004) 1102–1111.
[14] J. Fahrmeir, M. Gunther, N. Tietze, E. Wagner, M. Ogris, Electrophoretic purification of tumor-targeted polyethylenimine-based polyplexes reduces toxic side effects in vivo, J. Control. Release 122 (3) (2007) 236–245.
[15] T. Ito, N. Iida-Tanaka, Y. Koyama, Efficient in vivo gene transfection by stable DNA/PEI complexes coated by hyaluronic acid, J. Drug Target. 16 (4) (2008) 276–281.
[16] T. Ito, N. Iida-Tanaka, T. Niidome, T. Kawano, K. Kubo, K. Yoshikawa, T. Sato, Z. Yang, Y. Koyama, Hyaluronic acid and its derivative as a multi-functional gene expression enhancer: protection from non-specific interactions, adhesion to targeted cells, and transcriptional activation, J. Control. Release 112 (3) (2006) 382–388.
[17] T. Ito, C. Yoshihara, K. Hamada, Y. Koyama, DNA/polyethyleneimine/hyaluronic acid small complex particles and tumor suppression in mice, Biomaterials 31 (10) (2010) 2912–2918.
[18] T. Kurosaki, T. Kitahara, S. Kawakami, K. Nishida, J. Nakamura, M. Teshima, H. Nakagawa, Y. Kodama, H. To, H. Sasaki, The development of a gene vector electrostatically assembled with a polysaccharide capsule, Biomaterials 30 (26) (2009) 4427–4434.
[19] A. Pathak, P. Kumar, K. Chuttani, S. Jain, A.K. Mishra, S.P. Vyas, K.C. Gupta, Gene Expression, Biodistribution, and Pharmacoscintigraphic Evaluation of Chondroitin Sulfate-PEI Nanoconstructs Mediated Tumor Gene Therapy, ACS Nano (2009).
[20] P. Xu, G.K. Quick, Y. Yeo, Gene delivery through the use of a hyaluronate-associated intracellularly degradable crosslinked polyethyleneimine, Biomaterials 30 (29) (2009) 5834–5843.
[21] P.T. Vernier, Y. Sun, M.A. Gundersen, Nanoelectropulse-driven membrane perturbation and small molecule permeabilization, BMC Cell Biol. 7 (2006) 37.
[22] M. Oba, K. Miyata, K. Osada, R.J. Christie, M. Sanjoh, W. Li, S. Fukushima, T. Ishii, M.R. Kano, N. Nishiyama, H. Koyama, K. Kataoka, Polyplex micelles prepared from omega-cholesteryl PEG-polycation block copolymers for systemic gene delivery, Biomaterials 32 (2) (2011) 652–663.
[23] M. Ruponen, S. Yla-Herttuala, A. Urtti, Interactions of polymeric and liposomal gene delivery systems with extracellular glycosaminoglycans: physicochemical and transfection studies, Biochim. Biophys. Acta 1415 (2) (1999) 331–341.
[24] K. Itaka, A. Harada, K. Nakamura, H. Kawaguchi, K. Kataoka, Evaluation by fluorescence resonance energy transfer of the stability of nonviral gene delivery vectors under physiological conditions, Biomacromolecules 3 (4) (2002) 841–845.
[25] K. Itaka, A. Harada, Y. Yamasaki, K. Nakamura, H. Kawaguchi, K. Kataoka, In situ single cell observation by fluorescence resonance energy transfer reveals fast intra-cytoplasmic delivery and easy release of plasmid DNA complexed with linear polyethylenimine, J. Gene Med. 6 (1) (2004) 76–84.

JACS
JOURNAL OF THE AMERICAN CHEMICAL SOCIETY

ARTICLE

pubs.acs.org/JACS

Odd–Even Effect of Repeating Aminoethylene Units in the Side Chain of N-Substituted Polyaspartamides on Gene Transfection Profiles

Hirokuni Uchida,[†] Kanjiro Miyata,[§] Makoto Oba,[∥] Takehiko Ishii,[†] Tomoya Suma,[†] Keiji Itaka,[§] Nobuhiro Nishiyama,[§] and Kazunori Kataoka*[,†,§,‡]

[†]Department of Bioengineering and [‡]Department of Materials Engineering, Graduate School of Engineering, The University of Tokyo, 7-3-1 Hongo, Bunkyo, Tokyo 113-8656, Japan

[§]Center for Disease Biology and Integrative Medicine, Graduate School of Medicine, The University of Tokyo, 7-3-1 Hongo, Bunkyo, Tokyo 113-0033, Japan

[∥]Department of Clinical Vascular Regeneration, Graduate School of Medicine, The University of Tokyo, 7-3-1 Hongo, Bunkyo, Tokyo 113-8655, Japan

Supporting Information

ABSTRACT: A series of the N-substituted polyaspartamides possessing repeating aminoethylene units in the side chain was prepared in this study to identify polyplexes with effective endosomal escape and low cytotoxicity. All cationic N-substituted polyaspartamides showed appreciably lower cytotoxicity than that of commercial transfection reagents. Interestingly, a distinctive odd–even effect of the repeating aminoethylene units in the polymer side chain on the efficiencies of endosomal escape and transfection to several cell lines was observed. The polyplexes from the polymers with an even number of repeating aminoethylene units (PA-Es) achieved an order of magnitude higher transfection efficiency, without marked cytotoxicity, than those of the polymers with an odd number of repeating aminoethylene units (PA-Os). This odd–even effect agreed well with the buffering capacity of these polymers as well as their capability to disrupt membrane integrity selectively at endosomal pH, leading to highly effective endosomal escape of the PA-E polyplexes. Furthermore, the formation of a polyvalent charged array with precise spacing between protonated amino groups in the polymer side chain was shown to be essential for effective disruption of the endosomal membrane, thus facilitating transport of the polyplex into the cytoplasm. These data provide useful knowledge for designing polycations to construct safe and efficient nonviral gene carriers.

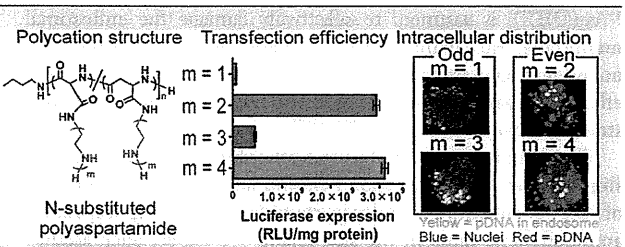

INTRODUCTION

Gene therapy has received considerable attention because of its significant potential to treat intractable diseases; however, the development of safe and efficient carriers of plasmid DNA (pDNA) remains a critical issue.[1,2] Among pDNA carriers, polyion complexes (PICs) formed between negatively charged DNA and polycations, which are termed "polyplexes", have been extensively studied.[3−8] Such polyplexes are required to stably deliver pDNA to the nuclei in the target cells. However, the most critical issue affecting the trafficking of polyplexes is the inefficient translocation from the endosomes to the cytoplasm after internalization through the endocytosis.[9] Hence, considerable efforts have been devoted to the development of polycations with potent endosomal escape ability.[10−15] However, such polycations often cause severe cytotoxicity.[16] Therefore, the fine-tuning the chemical structures of polycations to enhance their endosomal escape ability while cytotoxicity is reduced is a major key in designing polyplexes; this proves to be a challenge with respect to various fields of chemistry.

Linear polyethylenimine (linear PEI) is one of the most widely used polycations possessing potent endosomal escape ability.[17−20] Indeed, linear PEI polyplexes have been examined in several disease models to evaluate their clinical applications.[21] Linear PEI consists of repeating aminoethylene units and features a relatively low pK_a.[22] Hence, the protonation degree of linear PEI increases when pH decreases from the extracellular pH (~7.4) to the endosomal pH (~5.5). This facilitates the endosomal escape of linear PEI polyplexes because of endosomal disruption caused by increased osmotic pressure in the endosome (the so-called proton sponge effect[12,17]) and/or perturbation of the endosomal membrane caused by a direct interaction with polycations.[23−26] Thus, linear PEI exhibits a relatively high transfection efficiency but consequently induces considerable cytotoxicity because of interactions with biomolecules including the plasma membrane.[16,27] In order to solve this cytotoxicity problem, we have truncated a defined number of repeating aminoethylene units and introduced them into the side chain of the N-substituted polyaspartamides to obtain fine-tuned polycations achieving efficient gene transfection but reduced cytotoxicity. In our previous study,

Received: May 16, 2011
Published: August 31, 2011

Scheme 1. Synthesis of PAsp(EDA), PAsp(DET), PAsp(TET), and PAsp(TEP) by Aminolysis of PBLA

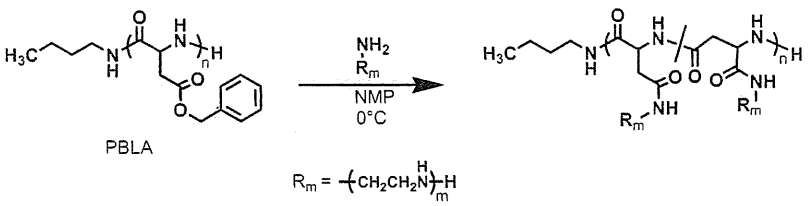

poly{*N*-[*N*′-(2-aminoethyl)-2-aminoethyl]aspartamide} possessing two repeating aminoethylene units [−(CH_2−CH_2−NH)$_2$−H] was synthesized by the introduction of diethylenetriamine (DET) (bis(2-aminoethyl)amine) [PAsp(DET)] into the side chain of the N-substituted polyaspartamide.[28] PAsp(DET) showed minimal membrane destabilizing ability with a monoprotonated side chain at pH 7.4 but a potent membrane destabilizing effect with a diprotonated side chain at pH 5.5. Thus, PAsp(DET) is assumed to selectively damage the endosomal membrane, thus enabling less toxic gene transfer in various cells including fragile primary culture cells.[26] Furthermore, the in vivo efficacy of gene transfer using PAsp(DET) has been demonstrated in several disease models.[29,30]

These studies motivated us to further investigate the relationship between the protonation behavior and biological properties of the N-substituted polyaspartamides possessing repeating aminoethylene units in the side chain. We expect such studies to provide useful knowledge for designing polycations that are safe and efficient nonviral gene carriers. Therefore, in this study, we examined various N-substituted polyaspartamides possessing different numbers of repeating aminoethylene units in the side chain and evaluated the relationship between their protonated states at pH 7.4 and 5.5 and their biological properties such as the hemolytic activity, cytotoxicity, endosomal escape ability, and transfection efficiency. Interestingly, a distinctive odd−even effect associated with the number of aminoethylene units was observed on the efficiencies of endosomal escape and in vitro transfection. The polyplexes from the N-substituted polyaspartamides possessing even-numbered repeating aminoethylene units (PA-Es) achieved transfection efficiencies, without marked cytotoxicity, that were an order of magnitude higher than those from the N-substituted polyaspartamides possessing odd-numbered repeating aminoethylene units (PA-Os). The mechanism for endosomal escape of these N-substituted polyaspartamide polyplexes was examined in detail to explain this interesting odd−even effect.

RESULTS

Synthesis and Characterization of N-Substituted Polyaspartamides. Introduction of repeating aminoethylene units into the poly(β-benzyl-L-aspartate) (PBLA) side chain was performed by the aminolysis reaction of PBLA with ethylenediamine (EDA), diethylenetriamine (DET), triethylenetetramine (TET), or tetraethylenepentamine (TEP), as previously reported,[31] and we synthesized poly[*N*-(2-aminoethyl)aspartamide] [PAsp(EDA)], PAsp(DET), poly(*N*-{*N*′-[*N*″-(2-aminoethyl)-2-aminoethyl]-2-aminoethyl}aspartamide) [PAsp(TET)], and poly-[*N*-(*N*′-{*N*″-[*N*‴-(2-aminoethyl)-2-aminoethyl]-2-aminoethyl}-2-aminoethyl)aspartamide] [PAsp(TEP)] (Scheme 1). It is noteworthy that in this way a series of N-substituted cationic polyaspartamides, with the same polymerization degree and molecular weight distribution, was readily obtained.[32] Each N-substituted cationic polyaspartamide is abbreviated as PAsp-(R), in which R denotes the abbreviation of the amines substituted in the side chain. The quantitative aminolysis of the side chain was confirmed from the peak intensity ratio of the protons from the methyl group at the α-chain end of the polymer ($CH_3CH_2CH_2CH_2$−, δ = 0.9 ppm) to all the methylene protons in the side chains (δ = 2.7−3.6 ppm) in the ^{1}H NMR spectra (Figure 1).

pH-Dependent Change in the Degree of Protonation (α) of Amino Groups in the Side Chain of N-Substituted Polyaspartamides. In order to estimate the protonation states of the amino groups in the side chain of the N-substituted polyaspartamide (hereafter, the polymer), potentiometric titration was performed in the pH range 1.2−11.5 in a 150 mM NaCl solution at 37 °C. The resultant titration curves were converted to differential curves to determine each neutralization point (data not shown). The total molar amount of consumed NaOH in the titration of PAsp(EDA) and PAsp(DET) corresponded well to the residual molar amount of amino groups of each polymer (5 mmol) in the solution, indicating that all the amino groups of the polymer were protonated at the beginning (pH 1.2) and deprotonated at the end (pH 11.5). Accordingly, the degree of protonation (α) and pK (=pH + log[α/(1 − α)]) were calculated and plotted against pH and α, respectively (Figure 2). On the other hand, the molar amount of consumed NaOH for the titration of PAsp(TET) and PAsp(TEP) was substantially lower than the residual molar amount of amino groups in the solution, suggesting that the amino groups in PAsp(TET) and PAsp-(TEP) should not be fully protonated, even at pH 1.2. Thus, the α/pH and pK/α curves of these polymers were calculated from the neutralization point in the differential curve and also shown in Figure 2. The change in the degree of protonation between pH 7.4 and 5.5 ($\Delta\alpha$), indicating the buffering capacity, was calculated for each polymer from the values of α at pH 7.4 and 5.5 and is summarized in Table 1. Obviously, PAsp(DET) showed the largest $\Delta\alpha$, followed by PAsp(TEP), PAsp(TET), and PAsp-(EDA). The number of protonated amines in each polymer (NA) at the corresponding pH was also calculated from α and the number of residual amino groups in the polymer by the following equation: NA = $\alpha n \times 102$, where n is the repeating number of aminoethylene units in the polymer side chain and 102 is the averaged polymerization degree. Furthermore, the averaged cationic charge density (CD) of each polymer was defined as the ratio of the NA to the number-averaged molecular weight (M_n) of the polymers (Table 1). The pK_a values for each protonation step were determined from the pK/α curves and are summarized in Table 1. Note that the p$K_{a4,TEP}$ value was not determined because the fourth protonation of the residual amino

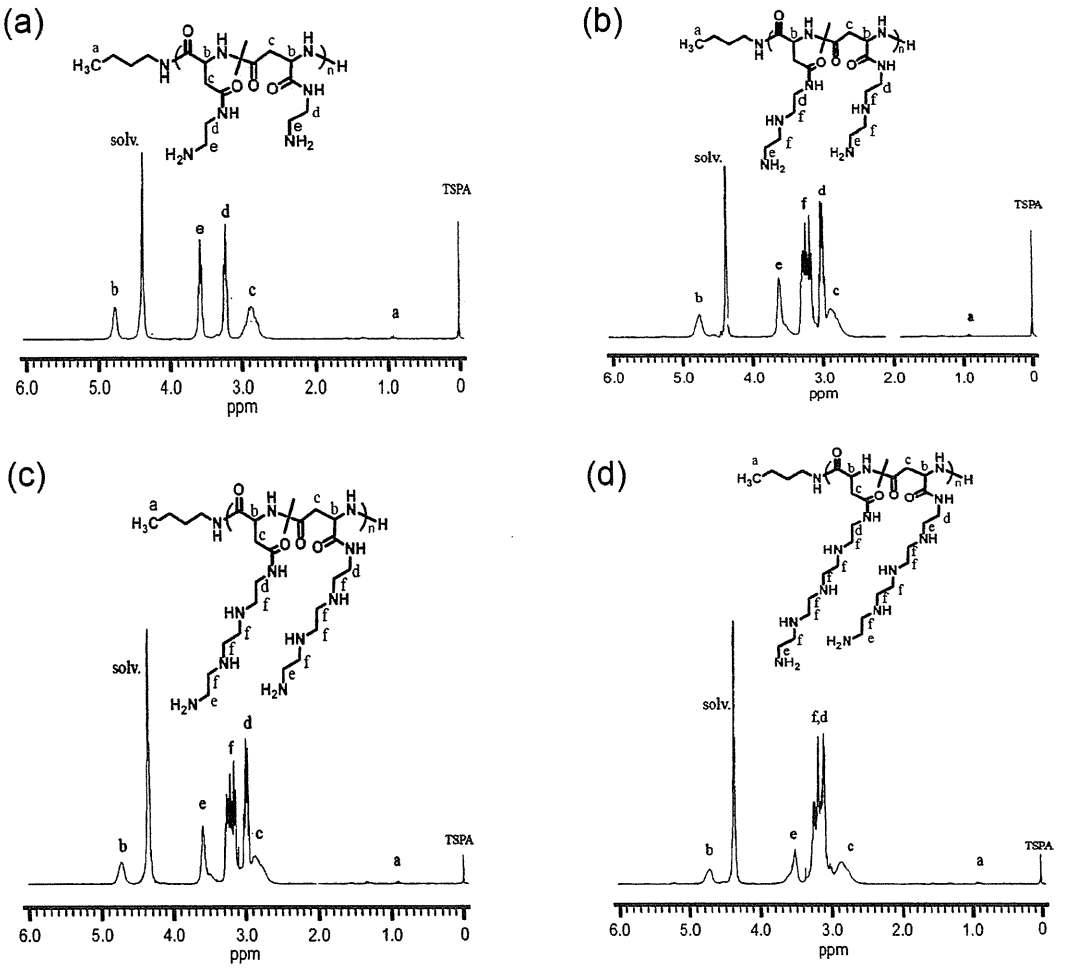

Figure 1. ^{1}H NMR spectra of (a) PAsp(EDA), (b) PAsp(DET), (c) PAsp(TET), and (d) PAsp(TEP). Solvent, D_2O; temperature, 70 °C; polymer concentration, 10 mg/mL.

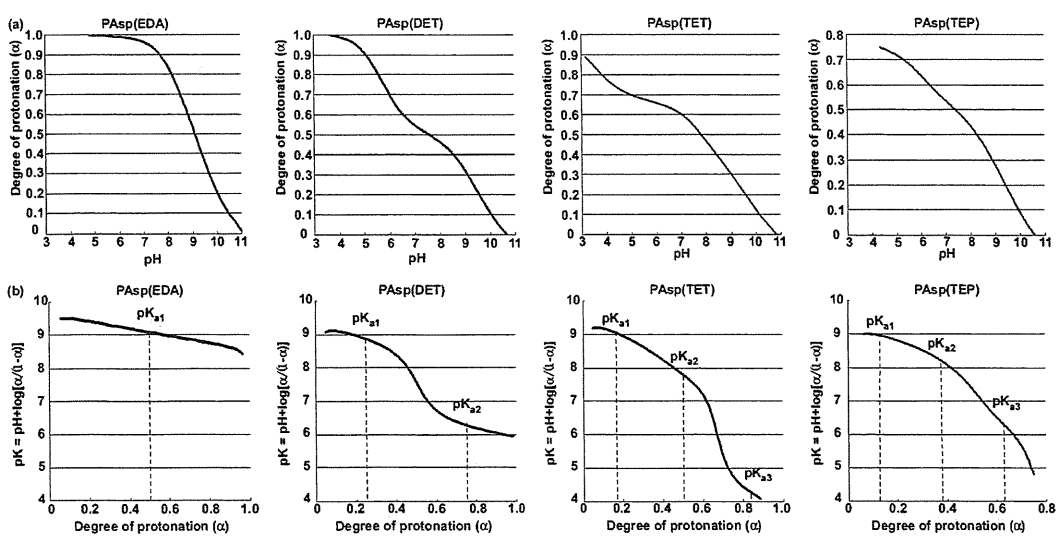

Figure 2. (a) α/pH curves and (b) pK_a/α curves of each N-substituted polyaspartamide in 150 mM NaCl solution at 37 °C.

Table 1. Physicochemical Parameters of the N-Substituted Polyaspartamides at pH 7.4 and 5.5

	α			number of protonated amines (NA[a])		charge density (CD[b])				
polymer	pH 7.4	pH 5.5	$\Delta\alpha$	pH 7.4	pH 5.5	pH 7.4	pH 5.5	pK_{a_1}	pK_{a_2}	pK_{a_3}
PAsp(EDA)	0.93	0.99	0.06	94	100	0.00538	0.00621	9.0		
PAsp(DET)	0.51	0.82	0.31	104	167	0.00505	0.00811	8.9	6.2	
PAsp(TET)	0.56	0.66	0.10	171	205	0.00682	0.00817	9.1	7.8	4.3
PAsp(TEP)	0.49	0.68	0.17	199	277	0.00673	0.00936	9.0	8.2	6.3

[a] NA = α × (the repeating number of aminoethylene units in the polymer side chain) × (the polymerization degree). [b] The ratio of the NA to the number-averaged molecular weight (M_n) of polymers.

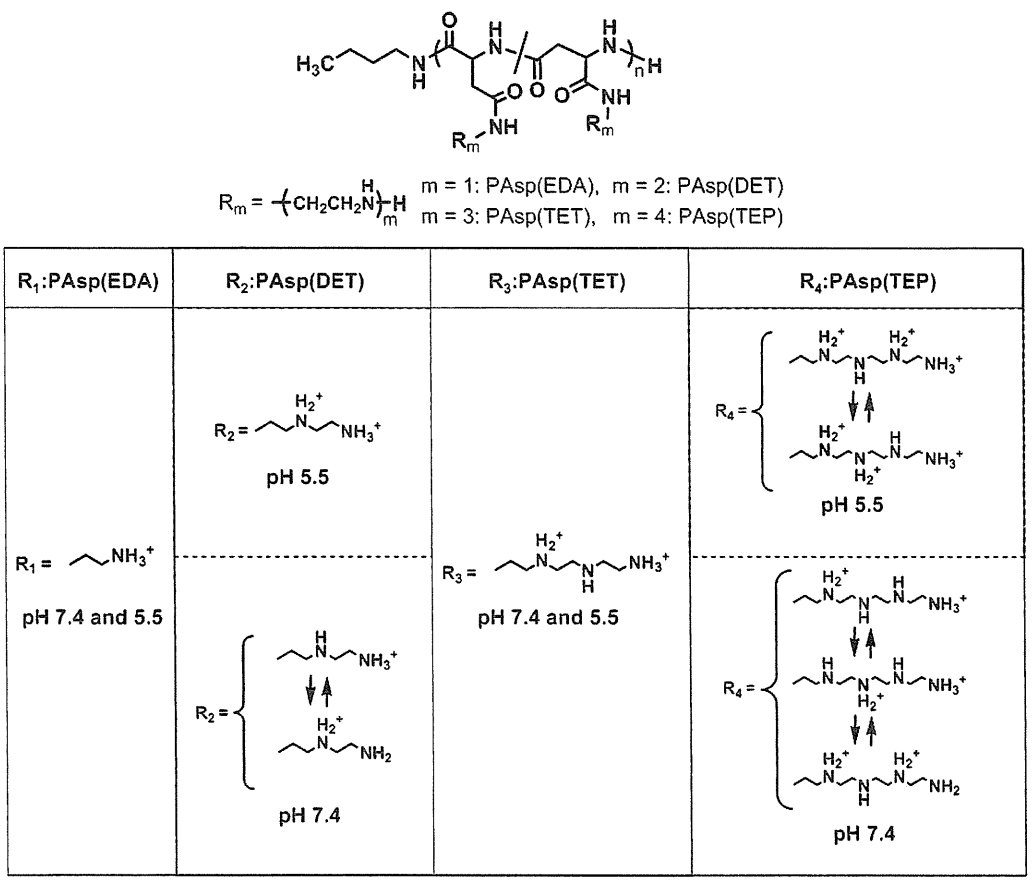

Figure 3. Major protonated structures of amino groups in the side chain of each polyaspartamide at pH 7.4 and 5.5.

groups in PAsp(TEP) was substantially limited, even at pH 1.2. Eventually, the major protonated structures of these polymers under physiological (pH = 7.4) and endosomal (pH = 5.5) conditions were estimated as shown in Figure 3.

Membrane Destabilizing Activity of N-Substituted Polyaspartamides. Our previous study revealed that PAsp(DET) disturbs the integrity of cellular membranes selectively at endosomal acidic pH presumably because of the transition of the side chain diamine unit from a monoprotonated to diprotonated state, which enhances the local charge density and facilitates the interaction with cellular membranes.[26] To determine the membrane-destabilizing activities of the N-substituted polyaspartamides as well as linear PEI (ExGen 500), the hemolysis assay was performed by mixing these polymers with murine erythrocytes at pH 7.4 and 5.5, at which extracellular neutral and endosomal acidic conditions, respectively, were simulated. As shown in Figure 4, ExGen 500 showed a considerably high hemolysis ratio (approximately 30%) at pH 7.4, which may be correlated with its high cytotoxicity. In contrast, all polymers induced substantially low hemolysis (less than 5%) at pH 7.4. Alternatively, at pH 5.5, the polymers possessing even-numbered repeating aminoethylene units [PAsp(DET) and PAsp(TEP)] and ExGen 500 significantly enhanced the hemolytic activity, whereas those possessing odd-numbered repeating units [PAsp(EDA) and PAsp(TET)] showed no significant increase. Thus, a unique odd–even effect of the repeating number of aminoethylene units was clearly observed for the pH-dependent hemolytic activity of a series of N-substituted polyaspartamides. Furthermore, the hemolytic

dx.doi.org/10.1021/ja204466y | J. Am. Chem. Soc. 2011, 133, 15524–15532

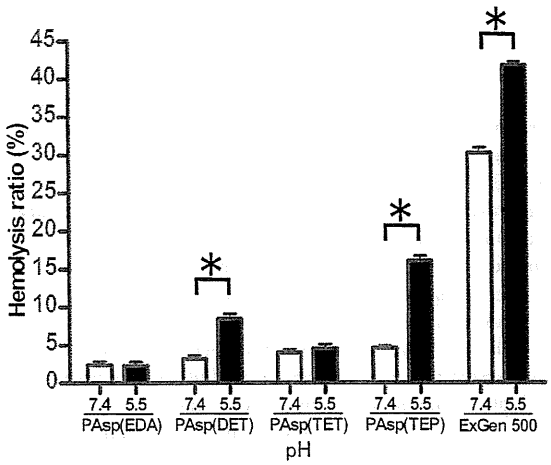

Figure 4. Hemolytic activity of PAsp(EDA), PAsp(DET), PAsp(TET), PAsp(TEP), and ExGen 500 ([amine] = 5 mM) against murine erythrocytes at pH 7.4 and 5.5. Results are expressed as mean ± SEM (N = 4). *P < 0.05.

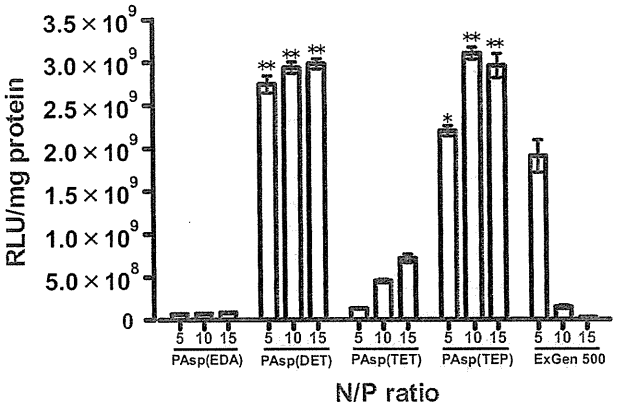

Figure 5. In vitro transfection efficiency of PAsp(EDA), PAsp(DET), PAsp(TET), PAsp(TEP), and ExGen 500 polyplexes at varying N/P ratios with Huh-7 cells determined by luciferase assay. Results are expressed as mean ± SEM (N = 4). * indicates that polyplexes show a significantly higher transfection efficiency than the PA-Os polyplexes at the same N/P ratio (P < 0.01), ** indicates that polyplexes show a significantly higher transfection efficiency than the PA-Os polyplexes at the same N/P ratio (P < 0.01) and the ExGen 500 polyplexes at N/P = 5 (P < 0.05).

activities of the polyplexes from the N-substituted polyaspartamides and ExGen 500 were determined at N/P = 10, which corresponds to the residual molar ratio of the amino groups in polycations to the phosphate groups in pDNA (Figure 1, Supporting Information). The hemolytic activity of polyplexes showed a similar odd–even effect, indicating that the membrane-destabilizing activity of the polycations was maintained even after the formation of polyplexes.

Size and ζ-Potential of Polyplexes Prepared from pDNA and N-Substituted Polyaspartamides. The polyplexes from the N-substituted polyaspartamides were characterized by measuring the ζ-potential and hydrodynamic diameter at pH 7.4 and 37 °C (Figure 2, Supporting Information). At N/P ratios above 4, all polyplexes had a similar size of approximately 100 nm with a

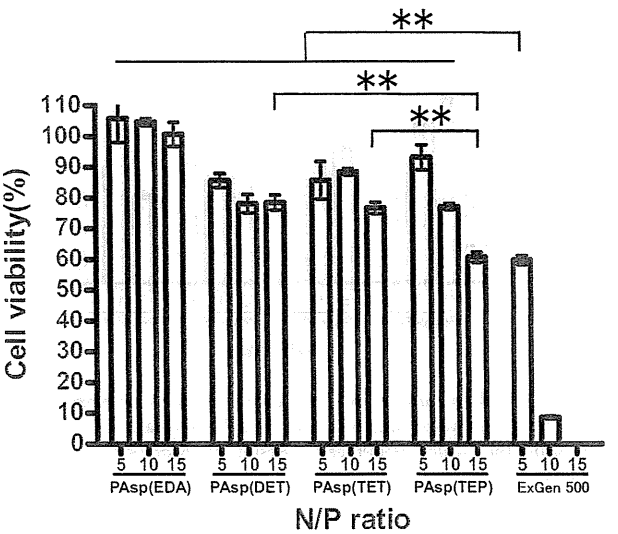

Figure 6. Cell viability assay of Huh-7 cells incubated with PAsp(EDA), PAsp(DET), PAsp(TET), PAsp(TEP), and ExGen 500 polyplexes under the same experimental conditions as in Figure 5. Results are expressed as mean ± SEM (N = 4). **P < 0.01.

constant ζ-potential of approximately 30 mV. Note that the formation of large aggregates around 1 μm was observed in each polyplex at a specific N/P ratio. Because each polyplex exhibited a ζ-potential close to neutral at this N/P ratio, large aggregate formation is expected to be due to decreased colloidal stability induced by charge neutralization. In the following experiments, the polyplexes prepared at N/P ratios above 4 were used because they apparently have similar physicochemical characteristics.

In Vitro Transfection and Cytotoxicity. The transfection efficiency of the luciferase gene in human hepatoma cells (Huh-7) was compared among the polyplexes prepared from PAsp(EDA), PAsp(DET), PAsp(TET), and PAsp(TEP) at N/P = 5, 10, and 15 (Figure 5). The polyplex from a linear PEI-based commercial transfection reagent (ExGen 500) was used as a control. Remarkable transfection efficiencies, which were higher than the maximum value obtained by ExGen 500 at N/P = 5, were achieved by polyplexes from PAsp(DET) (over N/P = 5) and PAsp(TEP) (over N/P = 10) possessing the even-numbered repeating aminoethylene units (PA-Es) (P < 0.05). Furthermore, polyplexes from PA-Es [PAsp(DET) and PAsp(TEP)] revealed significantly higher transfection efficiencies than those from PA-Os [PAsp(EDA) and PAsp(TET)] at all of the examined N/P ratios (P < 0.01). This remarkable odd–even effect on transfection efficiencies was not only limited to Huh-7 cells but was also observed for a human lung adenocarcinoma epithelial cells (A549) and a human umbilical vein endothelial cells (HUVEC) (Figure 3, Supporting Information). Note that a drastic reduction in the transfection efficiency was observed for the ExGen 500 polyplexes at higher N/P ratios, whereas it was not observed for any polyplexes from the N-substituted polyaspartamides. The substantially decreased transfection efficiency in the ExGen 500 polyplexes at higher N/P ratios is believed to be a direct result of severe cytotoxicity, as shown in Figure 6. In contrast, all polyplexes from the N-substituted polyaspartamides maintained a cell viability over 85% at N/P = 5 and over 75% even at N/P = 15, except for the polyplex from PAsp(TEP) at N/P = 15 (60%). Indeed, significant differences between the polyplexes from ExGen 500 at

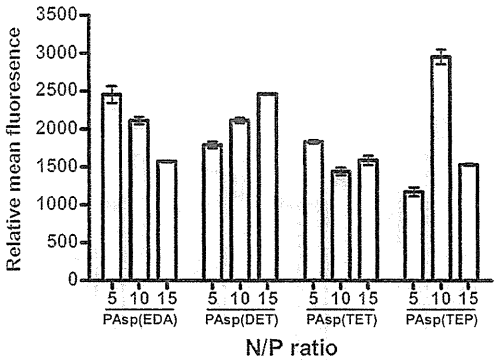

Figure 7. Cellular uptake of Cy5-labeled pDNA complexed with N-substituted polyaspartamides at various N/P ratios after 24 h incubation with Huh-7 cells (10 000 cells). Results are expressed as mean ± SEM (N = 4).

N/P = 5 and other N-substituted polyaspartamides except PAsp(TEP) at N/P = 15 were observed ($P < 0.01$). Polyplexes from PAsp(TEP) showed significantly lower cell viability than those from PAsp(DET) and PAsp(TET) at N/P = 15 ($P < 0.01$), indicating higher cytotoxicity with an increase in the N/P ratio.

Cellular Uptake of Polyplexes Determined by Flow Cytometry. The transfection efficiency of the polyplexes is often correlated with their cellular uptake. Thus, we compared the cellular uptake of each polyplex containing Cy5-labeled pDNA using flow cytometry. The histogram of flow cytometry revealed that almost 100% of the cells underwent polyplex uptake (data not shown). Figure 7 shows the relative mean fluorescence for the cellular uptake of Cy5-labeled pDNA, which apparently does not correlate with the transfection efficiency (Figure 5). Indeed, despite the significantly lower transfection efficiency, the polyplexes from PAsp(EDA) and PAsp(TET) showed levels of cellular uptake similar to those from PAsp(DET) and PAsp(TEP).

Intracellular Trafficking of Polyplexes Observed by Confocal Laser Scanning Microscopy (CLSM). Intracellular trafficking of each polyplex (N/P = 10) containing Cy5-labeled pDNA (red) was monitored particularly for endosomal localization by CLSM after staining the late endosome and lysosome with LysoTracker Green (green) and the nucleus with Hoechst 33342 (blue) (Figure 8a,b). In the overlay images, the yellow pixels represent the colocalization of Cy5-labeled pDNA with the late endosome/lysosome. Note that in our previous CLSM study Cy5-labeled pDNA in the poly(L-lysine) polyplex, which was used as the negative control and lacks endosomal escape ability, was found to maintain colocalization with the late endosome/lysosome throughout the observation period. This result provided the basis for estimating the endosomal escape ability of examined polyplexes from the decrease in the colocalization ratio estimated from the CLSM data.[26] Eventually, PAsp(DET) and PAsp(TEP) polyplexes appeared to disperse more efficiently in the entire cytoplasmic region than other polyplexes from the polymers with the odd-numbered repeating aminoethylene units in the side chains. As shown in Figure 8c, PAsp(EDA) and PAsp(TET) polyplexes showed an increase in the colocalization ratio until 12 and 24 h, respectively, indicating that the major fraction of PA-O polyplexes might be trapped in the lysosome. In contrast, PAsp(DET) and PAsp(TEP) polyplexes showed colocalization ratios lower than those of PAsp(EDA) and PAsp(TET) polyplexes at all time points. Also, PAsp(DET) and PAsp(TEP) polyplexes showed a decrease in the colocalization ratio after 12 and 6 h incubation, respectively, suggesting that the major fraction of PA-E polyplexes might escape from the endosome. At 12 h, the colocalization ratio of PAsp(DET) polyplexes was significantly lower than those of PAsp(EDA) and PAsp(TET) polyplexes ($P < 0.05$). At 24 and 48 h, the colocalization ratio of PAsp(TEP) polyplexes was significantly lower than that of PAsp(DET) polyplexes ($P < 0.05$ at 24 h, $P < 0.01$ at 48 h), indicating that the most efficient endosomal escape was for PAsp(TEP) polyplexes. Furthermore, the Manders coefficients were calculated using Image J software (http://rsbweb.nih.gov/ij/) to evaluate the colocalization of Cy5-labeled pDNA and LysoTracker after 48 h incubation. Note that the coefficients range between 0 and 1, which indicates no overlap and full overlap, respectively, and a higher value indicates that a larger fraction of polyplexes is trapped in the endosome/lysosome. The coefficients were calculated to be 0.549 for PAsp(EDA), 0.381 for PAsp(DET), 0.498 for PAsp(TET), and 0.345 for PAsp(TEP), consistent with the endosome colocalization ratios in Figure 8c. From these results, we conclude that the polyplexes from the polymer possessing the even-numbered repeating aminoethylene units enable the efficient endosomal escape of complexed pDNA into the cytoplasm, which agrees well with the transfection results shown in Figure 5.

DISCUSSION

In this study, to elucidate the precise structure–function relationship of the polyplexes, we synthesized a series of N-substituted polyaspartamides with increasing numbers of repeating aminoethylene units in the side chain: PAsp(EDA), PAsp(DET), PAsp(TET), and PAsp(TEP) (one to four repeating aminoethylene unit(s), respectively). The polyplexes from these N-substituted polyaspartamides were confirmed to have a similar size (~100 nm) and ζ-potential (~30 mV) at N/P ratios >4 (Figure 2, Supporting Information), suggesting similar fundamental physicochemical properties. The in vitro transfection experiment with Huh-7 cells exhibited a distinctive odd–even effect with respect to the number of repeating aminoethylene units: the polyplexes from the polymer with the even-numbered repeating aminoethylene units (PA-E) showed appreciably higher transfection efficiencies without marked cytotoxicity compared to polymers with odd-numbered repeating aminoethylene units (PA-O) (Figures 5 and 6).

To elucidate the reasons for this unique odd–even effect, we examined the cytotoxicity, cellular uptake, and endosomal escape behaviors of each polyplex. While the cell viability (Figure 6) and cellular uptake (Figure 7) profiles were similar between the polyplexes from both PA-E and PA-O, a significant difference in the endosomal escape behavior as determined from CLSM imagery was observed between the two variants. PA-E [PAsp(DET) and PAsp(TEP)] polyplexes revealed lower endosomal colocalization and higher dispersion into the cytoplasm than PA-O [PAsp(EDA) and PAsp(TET)] polyplexes (Figure 8), indicating that the higher transfection efficiency of the PA-E polyplexes is strongly correlated with their capability of endosomal escape.

Several previous studies revealed that the endosomal escape of the polyplexes may be facilitated by an increased osmotic pressure in the endosome because of a buffering effect associated with the amino groups in the constituent polycations (proton sponge hypothesis).[12,17] Accordingly, we examined the relationship between the buffering capacity of amino groups in the

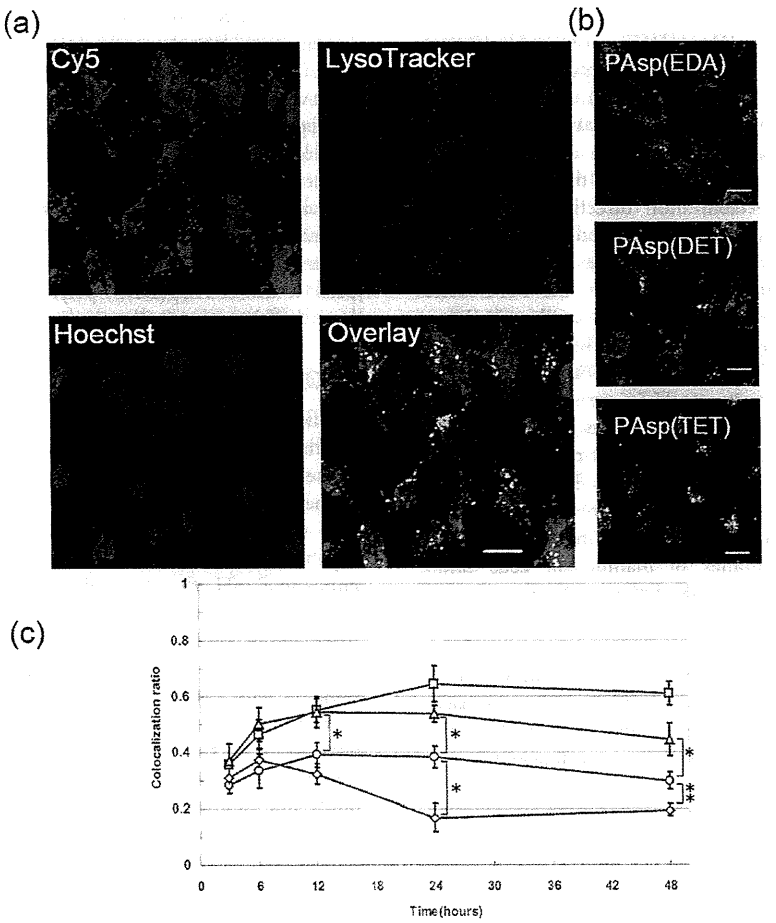

Figure 8. (a) Intracellular distribution of Cy5-labeled pDNA (red) complexed with PAsp(TEP) at N/P = 10 for Huh-7 cells after 48 h incubation. Acidic late endosomes and lysosomes were stained with LysoTracker Green (green). The nuclei were stained with Hoechst 33342 (blue). The scale bar represents 20 μm. (b) Overlay images of Cy5-labeled pDNA, LysoTracker Green, and Hoechst 33342 in Huh-7 transfected with the polyplexes from PAsp(EDA), PAsp(DET), and PAsp(TET) observed under the same conditions as those of part a. (c) Time-dependent changes in colocalization ratios of the PAsp(EDA) (square), PAsp(DET) (circle), PAsp(TET) (triangle), and PAsp(TEP) (diamond) polyplexes containing Cy5-labeled pDNA with late endosomes and lysosomes. Results are expressed as mean ± SEM (N = 10). $^*P < 0.05$, $^{**}P < 0.01$.

N-substituted polyaspartamides and the endosomal escape efficiency of their polyplexes. The buffering capacity was estimated from the change in the degree of protonation between pH 7.4 and 5.5 ($\Delta\alpha$) (Table 1) and was consistent with the observed odd–even effect. PA-Es [$\Delta\alpha$ = 0.31 and 0.19 for PAsp(DET) and PAsp(TEP), respectively] possess higher buffering capacities than PA-Os [$\Delta\alpha$ = 0.06 and 0.11 for PAsp(EDA) and PAsp(TET), respectively]. The assumed protonated structures of the side chains for each polymer (Figure 3) are rather interesting. Almost all the amino groups in the PAsp(EDA) side chains are protonated, regardless of pH (7.4 or 5.5). On the other hand, most of the PAsp(DET) side chains are in the monoprotonated state at pH 7.4 (α = 0.51) and diprotonated state at pH 5.5 (α = 0.82) owing to the appreciable difference in pK_{a_1} (8.9) and pK_{a_2} (6.2), as reported in our previous paper.[26] Low pK_{a_2} values in PAsp(DET) are due to the thermodynamic disadvantages of the diprotonated structure in 1,2-diaminoethane caused by electrostatic repulsion between the two protonated amines, locking the conformation in the *anti* form with less rotational freedom (butane effect). The absence of a significant change in α for PAsp(TET) with pH ($\Delta\alpha$ = 0.11) may be explained in a similar way: the fully protonated (triprotonated) structure of an *N*-(2-aminoethyl)-1,2-diaminoethane unit has a substantial thermodynamic penalty because of the strong repulsive force from the two neighboring protonated amines. Consequently, the side chain prefers to exist as a diprotonated structure with diethyleneamine spacing ($-NH_2^+-CH_2-CH_2-NH-CH_2-CH_2-NH_3^+$) containing a nonprotonated amino group in the center even at lower pH. Alternatively, for PAsp(TEP), α increases from 0.49 to 0.68 with a decrease in pH from 7.4 to 5.5 because the pK_{a_3} value (6.3) exists between these two pH values. As shown in Figure 3, the dominant structure changes from a diprotonated state at pH 7.4 to a triprotonated state at pH 5.5. The latter form, with its integrated positive charge, is still allowed under acidic conditions possibly because the increase in electrostatic repulsion accompanying the third protonation may be alleviated by sufficient length and rotational flexibility of the diethyeleneamine spacing ($-CH_2CH_2NHCH_2CH_2-$). Note that pK_{a_4} of PAsp(TEP) is much lower than the titration range (pH < 1.2) because of the highly repulsive nature of the fully protonated structure.

Although the buffering capacity may explain the odd–even effect observed in the transfection efficiency of the examined

polyplexes, it does not completely agree with the order of their endosomal escape efficiency. PAsp(DET) possessed relatively larger $\Delta\alpha$ than PAsp(TEP); however, the polyplex from the latter achieved significantly higher endosomal escape efficiency (lower endosomal colocalization ratio) than that from the former (Figure 8), suggesting the presence of an additional factor affecting the endosomal escape behavior of the polyplexes. In this regard, membrane destabilization directly by polycation interaction should be emphasized, as indicated from the result of the hemolysis assay shown in Figure 4. The odd−even effect was clearly observed in this assay and only the PA-E series induced a substantial increase in hemolysis at acidic pH. PAsp(TEP) demonstrated the highest hemolysis (14.4%), followed by PAsp(DET) (8.0%), PAsp(TET) (4.9%), and PAsp(EDA) (1.8%). The order of hemolytic activity at pH 5.5 agrees well with the endosomal escape efficiency of the polyplexes (Figure 8), suggesting that disturbing the membrane integrity may be important for the endosomal escape of these polyplexes. Furthermore, the weak hemolytic activity for each polymer at pH 7.4 agrees with their low cytotoxicity (Figure 6), suggesting their limited interaction with plasma membranes of mammalian cells under physiological conditions. Note that ExGen 500 also showed the membrane destabilizing activity in response to the acidic pH in the endosome (Figure 4). Nevertheless, it is assumed that the considerably high hemolytic activity (approximately 30%) of ExGen 500 at pH 7.4 may be correlated with its high cytotoxicity (Figure 6), suggesting that the augmentation of repeating aminoethylene units might increase cytotoxicity regardless of pH.

To further discuss the mechanism for cellular membrane destabilization induced by the N-substituted polyaspartamides, we focus here on the number of protonated amines (NA) and the overall cationic charge density (CD) in each polymer strand (Table 1). A previous study revealed that polycations with larger NA and higher CD tend to induce stronger disturbances in the membrane integrity, presumably resulting from a higher affinity of the plasma membrane for positively charged components.[33] Yet the calculated NA and CD were apparently not correlated with the hemolytic activity and simply increased with the number of aminoethylene units without any odd−even effects.

Next, we investigated whether the protonation state of the N-substituted polyaspartamides (Figure 3) would contribute to the odd−even effect from the viewpoint of specific interactions that may lead to a disturbance in the membrane integrity. It is interesting to consider that PA-Es [PAsp(DET) and PAsp(TEP), Figure 3] at pH 5.5 contain a diprotonated state of the diaminoethane unit ($-NH_2^+-CH_2-CH_2-NH_2^+-$), corresponding to their strong hemolytic activity in acidic conditions. In contrast, no such structure is determined for PA-Os [PAsp(EDA) and PAsp(TET)] at either pH 7.4 nor 5.5 nor for PA-Es at pH 7.4, and eventually they have very limited hemolytic activity. In particular, for PAsp(TET) at pH 7.4/5.5 and PAsp(TEP) at pH 7.4, two protonated amines are spatially separated by diethyleneamine ($-CH_2-CH_2-NH-CH_2-CH_2-$) or *N,N'*-ethylene-1,2-diaminoethane ($-CH_2-CH_2-NH-CH_2-CH_2-NH-CH_2-CH_2-$) spacers. It is likely that a critical spacing length between the two protonated amino groups may exist in order to induce an effective membrane interaction. Note that an N-substituted polyaspartamide possessing a 1,3-diaminopropane unit ($-NHCH_2CH_2CH_2NH-$) in the side chain [PAsp(DPT)] assumed a fully protonated structure at pH 7.4/5.5 and induced substantial membrane destabilization of mammalian cells, as previously reported.[26] It can be assumed that two positively charged units may need to be close to each other via a spacing equivalent of approximately two or three methylene units to exert a strong interaction with cellular membranes. The additional positively charged unit in the side chain of PAsp(TEP), separated from the diprotonated diamine unit ($-NH_2^+-CH_2-CH_2-NH_2^+-$) by a flexible $-CH_2-CH_2-NH-CH_2-CH_2-$ spacer, may contribute further to enhance the binding affinity through the formation of a polyvalent charged array as multiple binding sites. This multiple binding scheme reasonably explains PAsp(TEP) polyplex's higher hemolysis efficiency as well as its enhanced endosomal escape capability compared to that of PAsp(DET) polyplex, even though the former has a lower buffering capacity than the latter.

CONCLUSION

Efficient transfection without severe cytotoxicity was achieved by the polyplexes from the N-substituted polyaspartamides possessing the even-numbered repeating aminoethylene units in their side chains [PAsp(DET) and PAsp(TEP)]. This agrees with their appreciably high buffering capacity as well as their capability to disturb the membrane integrity selectively at endosomal pH, thereby facilitating the endosomal escape of the polyplexes. Results of the hemolysis assay and the CLSM observations tracking subcellular distribution of the polyplexes suggest that two protonated amino groups may need to be tethered with critical spacing equivalent to approximately two or three methylene units to induce the strong interaction of polycations in the polyplexes with the endosomal membrane, leading to their effective transport into the cytoplasm. Importantly, fine-tuning of the number, spacing, and protonation status of repetitive amine units in the polycation side chain, as reported in this study, resolves the conflict between endosomal escape and cytotoxicity of the polyplexes, thus providing a new design concept for nonviral gene delivery systems directed toward clinical applications.

ASSOCIATED CONTENT

Supporting Information. Experimental Section and supplemental Figures 1−3. This material is available free of charge via the Internet at: http://pubs.acs.org

AUTHOR INFORMATION

Corresponding Author
kataoka@bmw.t.u-tokyo.ac.jp

ACKNOWLEDGMENT

This work was financially supported in part by the Center for Medical System Innovation (CMSI) and the Funding Program for World-Leading Innovative R&D on Science and Technology (FIRST) from Japan Society for the Promotion of Science (JSPS) and the Core Research Program for Evolutional Science and Technology (CREST) from Japan Science and Technology Agency (JST). The authors thank Kotoe Date (The University of Tokyo) for her technical assistance.

REFERENCES

(1) Mastrobattista, E.; van der Aa, M. A.; Hennink, W. E.; Crommelin, D. J. A. *Nat. Rev. Drug Discovery* **2006**, *5*, 115–121.
(2) Mintzer, M. A.; Simanek, E. E. *Chem. Rev.* **2009**, *109*, 259–302.

(3) Pack, D. W.; Hoffman, A. S.; Pun, S. *Nat. Rev. Drug Discovery* **2005**, *4*, 581–593.
(4) Wood, K. C.; Little, S. R.; Langer, R.; Hammond, P. T. *Angew. Chem., Int. Ed.* **2005**, *44*, 6704–6708.
(5) Zugates, G. T.; Anderson, D. G.; Little, S. R.; Lawhorn, I. E. B.; Langer, R. *J. Am. Chem. Soc.* **2006**, *128*, 12726–12734.
(6) Srinivasachari, S.; Fichter, K. M.; Reineke, T. M. *J. Am. Chem. Soc.* **2008**, *130*, 4618–4627.
(7) Green, J. J.; Langer, R.; Anderson, D. G. *Acc. Chem. Res.* **2008**, *41*, 749–759.
(8) Schaffert, D.; Troiber, C.; Salcher, E. E.; Frohlich, T.; Martin, I.; Badgujar, N.; Dohmen, C.; Edinger, D.; Klager, R.; Maiwald, G.; Farkasova, K.; Seeber, S.; Jahn-Hofmann, K.; Hadwiger, P.; Wagner, E. *Angew. Chem., Int. Ed.* **2011**, *50*, 1–4.
(9) Wattiaux, R.; Laurent, N.; Coninck, W. N.; Jadot, M. *Adv. Drug Delivery Rev.* **2000**, *41*, 201–208.
(10) Wagner, E.; Plank, C.; Zatloukal, K.; Cotton, M.; Birnstiel, M. L. *Proc. Natl. Acad. Sci. U. S. A.* **1992**, *89*, 7934–7938.
(11) Haensler, J.; Szoka, F. C. *Bioconjugate Chem.* **1993**, *4*, 372–379.
(12) Boussif, O.; Lezoualc'h, F.; Zanta, M. A.; Mergny, M. D.; Scherman, D.; Demeneix, B.; Behr, J. P. *Proc. Natl. Acad. Sci. U. S. A.* **1995**, *92*, 7297–7301.
(13) Midoux, P.; Monsigny, M. *Bioconjugate Chem.* **1999**, *10*, 406–411.
(14) Thomas, M.; Kilbanov, A. M. *Proc. Natl. Acad. Sci. U. S. A.* **2002**, *99*, 14640–14645.
(15) Kwon, E. J.; Bergen, J. M.; Pun, S. H. *Bioconjugate Chem.* **2008**, *19*, 920–927.
(16) Hunter, A. C. *Adv. Drug Delivery Rev.* **2006**, *58*, 1523–1531.
(17) Neu, M.; Fischer, D.; Kissel, T. *J. Gene Med.* **2005**, *7*, 992–1009.
(18) Ferrari, S.; Moro, E.; Pettenazzo, A.; Behr, J. P.; Zacchello, F.; Scarpa, M. *Gene Ther.* **1997**, *4*, 1100–1106.
(19) Wightman, L.; Kircheis, R.; Rossler, V.; Carotta, S.; Ruzicka, R.; Kursa, M.; Wagner, E. *J. Gene Med.* **2001**, *3*, 362–372.
(20) Itaka, K.; Harada, A.; Yamasaki, Y.; Nakamura, K.; Kawaguchi, H.; Kataoka, K. *J. Gene Med.* **2004**, *6*, 76–84.
(21) Densmore, C. L.; Kleinerman, E. S.; Gautam, S.; Jia, S. F.; Xu, B.; Worth, L, L.; Waldrep, J. C.; Fung, Y. K.; Ang, A, T.; Knight, V. *Cancer Gene Ther.* **2001**, *8*, 619–627.
(22) Smits, R. G.; Koper, G. J. M.; Mandel, M. *J. Phys. Chem.* **1993**, *97*, 5745–5751.
(23) Merdan, T.; Kunath, K.; Fischer, D.; Kopecek, J.; Kissel, T. *Pharm. Res.* **2002**, *19*, 140–146.
(24) Bieber, T.; Meissener, W.; Kostin, S.; Niemann, A.; Elsasser, H.-P. *J. Controlled Release* **2002**, *82*, 441–454.
(25) Walker, G. F.; Fella, C.; Pelisek, J.; Fahrmeir, J.; Boeckle, S.; Ogris, M.; Wagner, E. *Mol. Ther.* **2005**, *11*, 418–425.
(26) Miyata, K.; Oba, M.; Nakanishi, M.; Fukushima, S.; Yamasaki, Y.; Koyama, H.; Nishiyama, N.; Kataoka, K. *J. Am. Chem. Soc.* **2008**, *130*, 16287–16294.
(27) Moghimi, S. M.; Symonds, P.; Murray, J. C.; Hunter, A. C.; Debska, G.; Szewczk, A. *Mol. Ther.* **2005**, *11*, 990–995.
(28) Kanayama, N.; Fukushima, S.; Nishiyama, N.; Itaka, K.; Jang, W. D.; Miyata, K.; Yamasaki, Y.; Chung, U.; Kataoka, K. *ChemMedChem.* **2006**, *1*, 439–444.
(29) Itaka, K.; Ohaba, S.; Miyata, K.; Kawaguchi, H.; Nakamura, K.; Takato, T.; Chung, U.; Kataoka, K. *Mol. Ther.* **2007**, *15*, 1655–1662.
(30) Harada-Shiba, M.; Takamisawa, I.; Miyata, K.; Ishii, T.; Nishiyama, N.; Itaka, K.; Kangawa, K.; Yoshihara, F.; Asada, Y.; Hatakeyama, K.; Nagaya, N.; Kataoka, K. *Mol. Ther.* **2009**, *17*, 1180–1186.
(31) Arnida; Nishiyama, N.; Kanayama, N.; Jang, W.-D.; Yamasaki, Y.; Kataoka, K. *J. Controlled Release* **2006**, *115*, 208–215.
(32) Nakanishi, M.; Park, J.-S.; Jang, W.-D.; Oba, M.; Kataoka, K. *React. Funct. Polym.* **2007**, *67*, 1361–1372.
(33) Fisher, D.; Li, Y.; Ahlemeyer, B.; Kreglstein, J.; Kissel, T. *Biomaterials* **2003**, *24*, 1121–1131.

Journal of Controlled Release 151 (2011) 104–109

Contents lists available at ScienceDirect

Journal of Controlled Release

journal homepage: www.elsevier.com/locate/jconrel

Concept Paper

In situ quantitative monitoring of polyplexes and polyplex micelles in the blood circulation using intravital real-time confocal laser scanning microscopy

Takahiro Nomoto [a,1], Yu Matsumoto [b,c,d,1], Kanjiro Miyata [b], Makoto Oba [e], Shigeto Fukushima [f], Nobuhiro Nishiyama [b], Tatsuya Yamasoba [c], Kazunori Kataoka [a,b,f,*]

[a] *Department of Bioengineering, Graduate School of Engineering, The University of Tokyo, Japan*
[b] *Division of Clinical Biotechnology, Center for Disease Biology and Integrative Medicine, Graduate School of Medicine, The University of Tokyo, Japan*
[c] *Department of Otorhinolaryngology and Head and Neck Surgery, Graduate School of Medicine and Faculty of Medicine, The University of Tokyo, Japan*
[d] *Department of Otorhinolaryngology and Head and Neck Surgery, Mitsui Memorial Hospital, Japan*
[e] *Department of Vascular Regeneration, Division of Tissue Engineering, The University of Tokyo Hospital, Japan*
[f] *Department of Materials Engineering, Graduate School of Engineering, The University of Tokyo, Japan*

ARTICLE INFO

Article history:
Received 12 January 2011
Accepted 10 February 2011
Available online 3 March 2011

Keywords:
Intravital confocal microscopy
Polyplex
Polyethylene glycol
Block copolymer
Polymer micelle

ABSTRACT

Surface modification using poly(ethylene glycol) (PEG) is a widely used strategy to improve the biocompatibility of cationic polymer-based nonviral gene vectors (polyplexes). A novel method based on intravital real-time confocal laser scanning microscopy (IVRTCLSM) was applied to quantify the dynamic states of polyplexes in the bloodstream, thereby demonstrating the efficacy of PEGylation to prevent their agglomeration. Blood flow in the earlobe blood vessels of experimental animals was monitored in a noninvasive manner to directly observe polyplexes in the circulation. Polyplexes formed distinct aggregates immediately after intravenous injection, followed by interaction with platelets. To quantify aggregate formation and platelet interaction, the coefficient of variation and Pearson's correlation coefficient were adopted. In contrast, polyplex micelles prepared through self-assembly of plasmid DNA with PEG-based block catiomers had dense PEG palisades, revealing no formation of aggregates without visible interaction with platelets during circulation. This is the first report of *in situ* monitoring and quantification of the availability of PEGylation to prevent polyplexes from agglomeration over time in the blood circulation. This shows the high utility of IVRTCLSM in drug and gene delivery research.

1. Concept of new methodologies

Gene therapy offers a unique potential for the treatment of genetic and intractable diseases and for tissue engineering. Its success is dependent upon the development of useful gene vectors as well as application of a drug delivery system (DDS). Nonviral gene vectors are attractive alternatives to viral gene vectors because they are much simpler to produce, transport and store, and induce fewer immune responses. Cationic polymers that electrostatically interact with plasmid DNA (pDNA) have been widely studied as materials to construct nonviral gene vectors [1–5]. The cationic polymers most commonly used as gene vectors include branched polyethylenimine (BPEI), linear polyethylenimine, poly(L-lysine) (PLys), chitosan, and dendrimers [6]. These polymers form polyion complexes (polyplexes) with pDNA to successfully transfer it into cultured cells to induce appreciable level of gene expression. However, these polyplexes have biocompatibility problems for systemic application. Polyplexes usually require excess polycations to generate electrostatic repulsion for their increased solubility and colloidal stability. This eventually results in a shift of their surface charge to a positive value. This positive charge causes nonspecific interaction with anionic components in the body such as plasma proteins and blood cells, which might lead to severe adverse effects [7,8]. Attachment of hydrophilic polymers such as poly(ethylene glycol) (PEG) is called "PEGylation" and has often been used to shield nonviral gene vectors from undesired interaction in the blood. PEGylation also contributes to diminished uptake by the reticuloendothelial system or macrophages, and hence the half-life in blood circulation can be extended.

It is well documented that a PEG palisade prevents nonspecific interaction with biological components. However, *in situ* evaluation of

Abbreviations: PEG, poly(ethylene glycol); DDS, drug delivery system; pDNA, plasmid DNA; BPEI, branched polyethylenimine; PLys, poly(L-lysine); PEG-PLys, poly(ethylene glycol)-*b*-poly(L-lysine); PAsp(DET), poly{*N*-[*N*-(2-aminoethyl)-2-aminoethyl]aspartamide}; PEG-PAsp(DET), poly(ethylene glycol)-*b*-poly{*N*-[*N*-(2-aminoethyl)-2-aminoethyl] aspartamide}; IVRTCLSM, intravital real-time confocal laser scanning microscopy; CV, coefficient of variation; PCC, Pearson's correlation coefficient.

* Corresponding author at: Department of Materials Engineering, Graduate School of Engineering, The University of Tokyo, 7-3-1 Hongo, Bunkyo-ku, Tokyo 113-0033, Japan. Tel.: +81 3 5841 7138; fax: +81 3 5841 7139.
E-mail address: kataoka@bmw.t.u-tokyo.ac.jp (K. Kataoka).

[1] These authors equally contributed to this work.

0168-3659/$ – see front matter © 2011 Elsevier B.V. All rights reserved.
doi:10.1016/j.jconrel.2011.02.011